

Acyclic Boron-Containing π -Ligand Complexes: η^2 - and η^3 -Coordination Modes




David J. H. Emslie, Bradley E. Cowie, and Kristopher B. Kolpin*

Department of Chemistry, McMaster University, 1280 Main Street West, Hamilton, ON, L8S 4M1, Canada. Fax: (905)-522-2509; Tel: (905)-525-9140 x 23307. E-mail: emslie@mcmaster.ca

RECEIVED DATE

Abstract: Cyclic boron-containing π -ligands such as boratabenzenes and borollides are well established, in particular as supporting ligands. By contrast, the chemistry of acyclic boron-containing π -ligands has remained relatively unexplored, presumably in part due to the higher reactivity of acyclic π -ligands relative to cyclic analogues. This perspective is focused on the synthesis, structures and reactivity of isolated transition metal complexes bearing η^n -coordinated ($n = 2$ or 3) acyclic boron-containing ligands. Both monometallic and multimetallic compounds are included, and are discussed with an emphasis on metal–ligand and intraligand bonding and parallels with hydrocarbon π -ligand complexes.

Author Photographs and Biographies

	<p><i>David J. H. Emslie was born in Edinburgh, Scotland, in 1975 and obtained his BSc in Chemistry from the University of Bristol in 1996. He then studied with Prof. Neil G. Connelly at the University of Bristol, and received his Ph.D. degree in 2000. Following a postdoctoral fellowship with Prof. Warren E. Piers at the University of Calgary, he joined the Department of Chemistry at McMaster University in 2003 where he is currently an Associate Professor. His research interests are: (1) borane-functionalized late transition metal complexes, with particular emphasis on synthesis, bonding and catalysis, (2) ultra-rigid ligand actinide chemistry with a focus on catalysis, small molecule activation, and lanthanide/actinide separation, and (3) the development of new organometallic reactivity for metal atomic layer deposition.</i></p>
	<p><i>Bradley E. Cowie was born in 1986 in Hamilton, Ontario. He received his B.Sc. in Chemistry from McMaster University in 2008, and is currently a Ph.D. student in the Emslie group. His research is focused on late transition metal complexes of boron-containing ambiphilic ligands.</i></p>
	<p><i>Kristopher B. Kolpin was born in 1986 in Hamilton, Ontario. In 2008, he received his B.Sc. in Chemistry from Trent University, and he is currently a Ph.D. student in the Emslie group. His research is focused on the synthesis, structures and reactivity of late transition vinylborane complexes.</i></p>

1 Introduction

Cyclic boron-containing π -ligands such as boratabenzenes and borollides (Figure 1) are well established, in particular as supporting ligands,¹ and relative to hydrocarbon π -ligands they offer new opportunities for modification of the electronic environment at a coordinated metal, not least due an increase in the negative charge on the ligand with each substitution of a CH group for an isoelectronic BH^- unit. By contrast, the chemistry of acyclic boron-containing π -ligands (Figure 1) has remained relatively unexplored, presumably in part due to the higher reactivity of acyclic π -ligands relative to cyclic analogues.

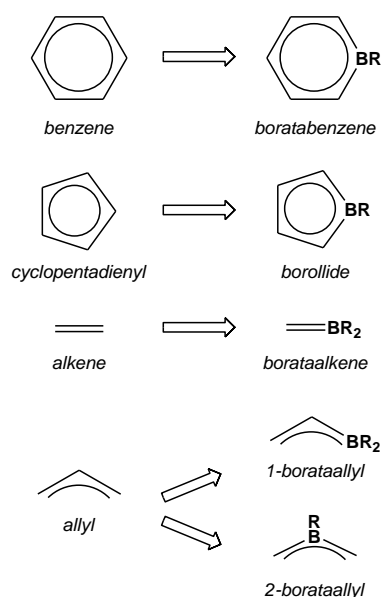


Figure 1. Selected cyclic and acyclic boron-containing π -ligands and their relationship to isostructural hydrocarbon π -ligands (charges are not assigned).

A large number of boron-containing ligands can be envisaged based on the acyclic hydrocarbon π -ligand structure types in Figure 2, and taking into account the potential for placement of boron at various positions in each ligand (e.g. in the central or terminal positions of an allyl ligand). This perspective is focused on transition metal complexes bearing η^2 - or η^3 -coordinated boron-containing acyclic π -ligands. η^2 -Coordinated complexes are discussed prior to η^3 -coordinated complexes, and in each section, monometallic complexes are described before bimetallic or cluster compounds. Complexes

bearing ligands containing elements other than boron and carbon within the η^n -coordinated unit, and most metallacarborane compounds are outside of the scope of this review.

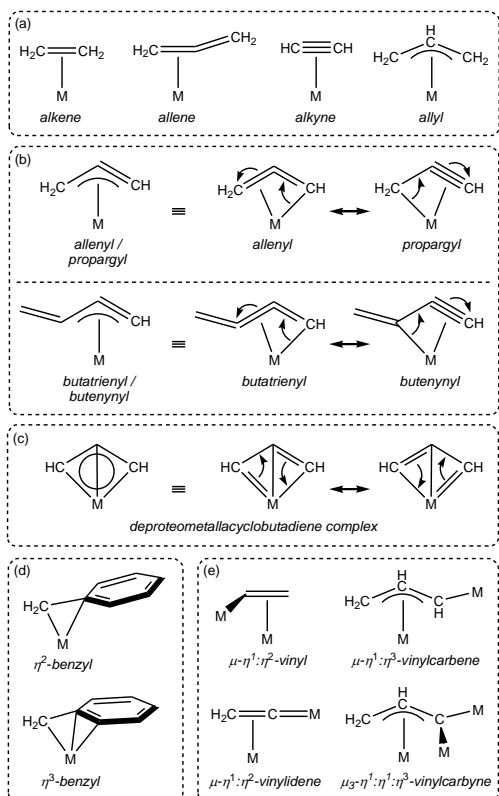


Figure 2. A selection of η^2 - and η^3 -coordinated acyclic hydrocarbon π -ligands from which boron-containing analogues may be derived. (a) Simple alkene (C_2H_4), allene (C_3H_4), alkyne (C_2H_2) and allyl (C_3H_5) ligands,^{2,3} (b) η^3 -coordinated ligands with non-equivalent resonance structures: allenyl/propargyl (C_3H_3) and butatrienyl/butenynyl (C_4H_3) ligands,^{4,5} (c) the C_3H_2 ligand in a deproteometallacyclobutadiene complex,^{6,7} (d) η^2 - and η^3 -benzyl ligands,^{2,3} and (e) μ - η^1 : η^2 -, μ - η^1 : η^3 - and μ_3 - η^1 : η^1 : η^3 -coordinated ligands.

2 Characterization of Acyclic Boron-Containing π -Ligands

2.1 Crystallographic Characterization

In boron-containing π -ligand complexes, M–C, M–B, C–C and B–C bond lengths can provide vital insight into the metal–ligand⁸ and intraligand bonding situation, although it is important to bear in mind that π -coordination can greatly reduce intraligand bond orders. Table 1 lists B–C bond distances for selected organoboron compounds, and these data define the following approximate B–C multiple bond distance ranges: (1) B=C double bonds in anionic $R_2C=BR_2^-$, $R_2C=B=CR_2^-$ and $R_2B=C=BR_2^{2-}$

compounds = 1.51–1.42 Å, (2) B=C double bonds in neutral R₂C=BR, R₂C=BR(L) and R₂C=B=NR₂ compounds = 1.43–1.36 Å, and (3) B≡C triple bonds in anionic RC≡BR⁻ compounds ≈ 1.32 Å. For the purpose of comparison, Table 1 also provides B–C_{sp}, B–C_{sp2} and B–C_{sp3} single bond lengths for selected 4-coordinate borane adducts (BR₃L) and 3-coordinate borane Lewis acids (BR₃; R = alkyl, aryl, vinyl or alkynyl).

Compound ^a	B–C distance (Å)	δ ¹¹ B NMR (ppm)	Ref.
BPh ₃ (THF)	1.626(4), 1.620(4), 1.619(4)	n.a.	9
B(C≡C ⁻ Bu) ₃ (THF)	1.580(1), 1.578(1), 1.575(1)	-8	10
BPh ₃	1.589(5), 1.571(3)	60	11
BEt ₃	1.573(1)	80	12
E–Mes ₂ B–CH=CHPh	1.554(2) for B–C _{vinyl} {1.577(2) for B–C _{Mes} }	n.a.	13
Mes ₂ B–C≡C–Mes	1.529(6) for B–C _{alkynyl} {1.599(6), 1.594(6) for B–C _{Mes} }	n.a.	14
B(C≡C ⁻ Bu) ₃	1.519(2)	38	10
Zwitterionic Mes ₂ B=C(SiMe ₃)–PF(N ⁱ Pr ₂) ₂ ^b	1.525(4)	63.5	15
[Li(12-C-4) ₂][Mes ₂ B=C ₆ H ₂ Me ₂ =CH ₂] ^c	1.522(10)	n.a.	16
Li ₂ [(Me ₃ Si) ₂ C=B(Mes)–B(Mes)=C(SiMe ₃) ₂]	1.509(8), 1.475(8)	57	17
Li ₂ (OEt ₂) ₃ [(SiMe ₃ CH ₂) ₂ B{(Me ₃ Si)C=B(Duryl)} ₂ O]	1.50(1), 1.514(9)	61, 42	18
[Li(tmeda) ₂][MesB=C ₆ H ₂ Me ₃ (C ₁₀ H ₆)]	1.475(6)	45	19
[K(dibenzo-18-C-6)(THF) ₂][MeN(C ₆ H ₄) ₂ C=BMes ₂]	1.462(8)	40	20
[Li(12-C-4) ₂][H ₂ C=BMes ₂]	1.438(9)	35	21
Li[(Me ₃ Si) ₂ C=B=C(BDuryl) ₂ {B(Duryl)(^t Bu)}]	1.45(1), 1.42(1)	75, 71	17
Li ₂ (toluene)[(Me ₃ Si) ₂ C=B(Duryl)–C ₆ HMe ₄ =B=C(SiMe ₃) ₂]	1.40(2) (R ₂ C=BR ₂ ⁻), 1.42(2), 1.39(2) (R ₂ C=B=CR ₂ ⁻)	63, 41	17
Li ₂ (OEt ₂) ₂ [Ar ₂ B=C=BAR ₂]; BAR ₂ = B(Duryl) ₂	1.465(1)	28	22
Li ₂ (OEt ₂) ₂ [Ar ₂ B=C=BAR ₂]; BAR ₂ = B(C ₆ H ₂ Me ₃ -2,4,5)(Duryl)	1.458(7), 1.468(7)	27	22
Li ₂ (OEt ₂) ₂ [(Mes)(^t Bu)B=C=B(^t Bu)(Mes)]	1.450(5)	32	23
(Me ₃ Si) ₂ C{B(Duryl)} ₂ C=B(Duryl)(OEt ₂)	1.431(8)	n.a.	24
(Mes ₂ B)(Me ₃ Sn)C=B(dmap)–CH(SiMe ₃) ₂	1.43(2)	63, 43	25
(C ₆ H ₄) ₂ C=B=NR ₂ (NR ₂ = tetramethylpiperidiny)	1.424(3), 1.420(3)* 2 mol in unit cell	59	26
(Me ₃ Si) ₂ C=B=N ⁱ Pr ₂	1.391(4)	46	27
Me(Duryl)B–C{CMe(SiMe ₂ Cl) ₂ }=B(Duryl)	1.404(9)	62	28
[(Me ₃ Si) ₂ C=C=C(CH ₂ ^t Bu)–B(Duryl)–C(CH ₂ ^t Bu)=B(Duryl)]	1.391(3)	60	29
(MesO) ₂ B–C{CH(SiMe ₃) ₂ }=B(Duryl)	1.384(11)	34 (BR ₃), 80 (R ₂ C=BR)	28
Me ₃ SiCH=CH–B(Duryl)–C(SiMe ₃)=B(Duryl)	1.379(3)	69	30
(Me ₃ Si) ₂ C{B(Duryl)} ₂ C=B(Duryl)	1.374(8)	71, 62	24
(DippO)(Duryl)B–C{CH(SiMe ₃) ₂ }=B(Duryl)	1.372(9)	47 (BR ₃), 79 (R ₂ C=BR)	28
Me(Duryl)B–CMe ₂ –B=C(SiMe ₃){SiMe ₂ (Duryl)}	1.363(9)	86, 69	31
(Me ₃ Si) ₂ C=B– ^t Bu	1.361(5)	70	32
(Mes ₂ B)(Me ₃ Sn)C=B–CH(SiMe ₃) ₂	1.31(1)	65, 52	25
Li ₂ (OEt ₂) ₂ [(Duryl)B≡C–B(Duryl)=C(SiMe ₃) ₂]	1.323(9) for RB≡CR ⁻ {1.505(9) for R ₂ C=BR ₂ ⁻ }	n.a.	33

(a) Mes = 2,4,6-trimethylphenyl, Duryl = 2,3,5,6-tetramethylphenyl, Dipp = 2,6-diisopropylphenyl.

(b) an alternative resonance structure is the ylide Mes₂B–C(SiMe₃)=PF(NⁱPr₂)₂.

(c) an alternative resonance structure is the Mes₂B–C₆H₂Me₂–CH₂ carbanion.

Table 1. B–C bond distances and ¹¹B NMR chemical shifts for selected neutral and anionic organoboron compounds (n.a. = not available).

2.2 NMR Spectroscopic Characterization

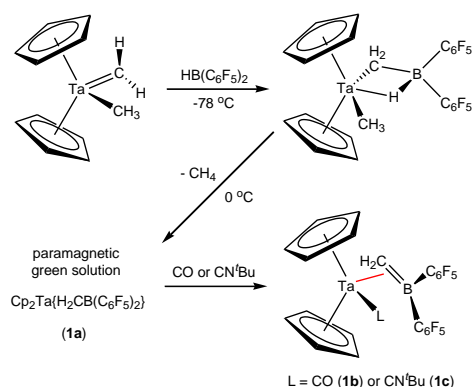
A key spectroscopic parameter for classification of transition metal-borane compounds (L_xM–BR₃) is their ¹¹B NMR chemical shift; tight coordination of the borane results in a substantial shift of the ¹¹B

NMR resonance to low frequency relative to the free ligand, regardless of whether the borane undergoes pyramidalization or remains planar.³⁴ For other ligands containing boron bound to three substituents (e.g. borataalkene, boratavinyl and boratavinylidene ligands), metal–boron coordination may similarly contribute towards low frequency shifts in the ¹¹B NMR resonances. However, the situation is less clear-cut since changes in the intraligand π -bond order will also have a substantial influence on ¹¹B NMR chemical shifts. In complexes containing C₆F₅ groups on boron, the ¹⁹F chemical shift difference for the *para* and *meta* signals ($\Delta\delta_{p,m}$) of the C₆F₅ rings can also be used to probe the coordination number at boron; larger $\Delta\delta_{p,m}$ values are typically observed for 3-coordinate boron compounds relative to 4-coordinate boranes and borates (e.g. $\Delta\delta_{p,m}$ = 17 ppm in B(C₆F₅)₃,³⁵ 7 ppm in B(C₆F₅)₃(THF)³⁶ and 4 ppm in B(C₆F₅)₄⁻).³⁷ NMR coupling of ligand boron or carbon atoms with metal (e.g. ⁸⁹Y, ¹⁰³Rh, ¹⁰⁷Ag, ¹⁰⁹Ag, ¹⁸⁹W and ¹⁹⁵Pt) or co-ligand (e.g. ³¹P) nuclei can also be particularly informative.

3 Complexes with η^2 -Coordinated BC Units

3.1. Borataalkene Complexes, Borylmetallocenes, and η^2 -Coordinated Arylboranes.

Alkenes are among the simplest π -hydrocarbon ligands, and their direct boron analogues are anionic borataalkene ligands (R₂C=BR₂⁻). In 2001 and 2002, Piers et al. reported the reaction of [Cp₂Ta(=CH₂)(CH₃)] with HB(C₆F₅)₂ to form [Cp₂Ta(CH₃){CH₂B(C₆F₅)₂(μ -H)}], which reductively eliminates methane above -20 °C. The green paramagnetic product of this reaction is formulated as [Cp₂Ta{H₂CB(C₆F₅)₂}] (**1a**) on the basis of computational studies and trapping experiments; in the presence of CO or CN^tBu, [Cp₂Ta(CH₃){CH₂B(C₆F₅)₂(μ -H)}] cleanly reacts to form diamagnetic [Cp₂Ta{ η^2 -H₂C=B(C₆F₅)₂}(CO)] (**1b**) and [Cp₂Ta{ η^2 -H₂C=B(C₆F₅)₂}(CN^tBu)] (**1c**), respectively (Scheme 1).^{38,39} Both **1b** and **1c** (Figure 3) were crystallographically characterized, and alkene-like bonding is supported by: (1) Ta–CH₂ distances of 2.337(5) and 2.348(5) Å, which are slightly longer than a typical Ta–C σ -bond, (2) Ta–B distances of 2.728(6) and 2.738(6) Å, (3) Ta–CH₂-B angles less than 90°, (4) B–C bond lengths of 1.508(8) and 1.525(7) Å, which are intermediate between the values expected for B–C_{sp3} and B=C_{sp2} bonds, (5) C≡O or C≡N stretching frequencies that are higher than would be expected for [Cp₂TaR(L)] (R = a conventional hydrocarbyl donor) derivatives, (6) low frequency ¹¹B NMR chemical shifts of 7.2 and 8.5 ppm, which are inconsistent with a free 3-coordinate borane, and (7) a difference in the ¹⁹F NMR chemical shifts for the *meta* and *para* C₆F₅ fluorine atoms ($\Delta\delta_{m,p}$) of 5.1 and 5.4 ppm. The boron atoms in **1b** and **1c** are also slightly pyramidalized { $\Sigma(\text{C–B–C}) = 354^\circ$ in both complexes}.



Scheme 1. Synthesis of $[\text{Cp}_2\text{Ta}\{\text{CH}_2\text{B}(\text{C}_6\text{F}_5)_2\}]$ (**1a**), $[\text{Cp}_2\text{Ta}\{\eta^2\text{-H}_2\text{C}=\text{B}(\text{C}_6\text{F}_5)_2\}(\text{CO})]$ (**1b**) and $[\text{Cp}_2\text{Ta}\{\eta^2\text{-H}_2\text{C}=\text{B}(\text{C}_6\text{F}_5)_2\}(\text{CN}^t\text{Bu})]$ (**1c**).

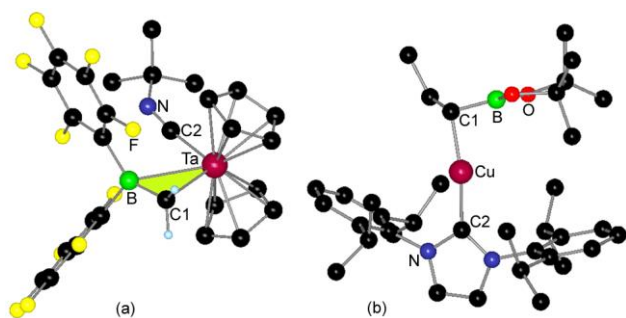
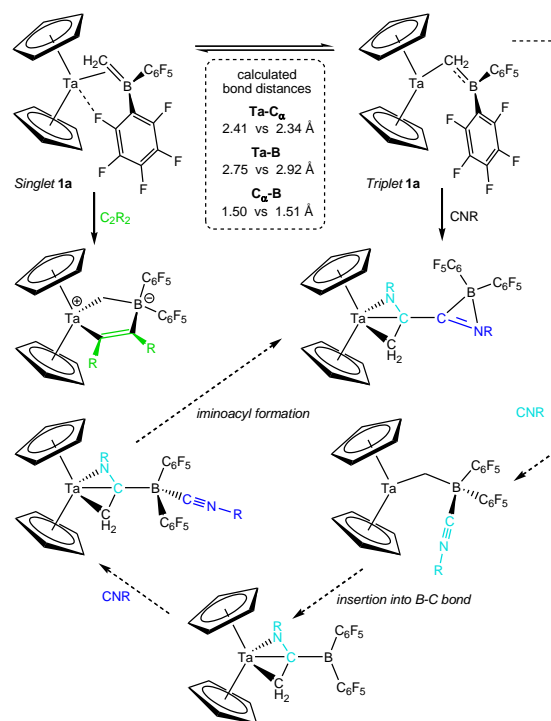


Figure 3. X-ray crystal structure of $[\text{Cp}_2\text{Ta}\{\eta^2\text{-H}_2\text{C}=\text{B}(\text{C}_6\text{F}_5)_2\}(\text{CN}^t\text{Bu})]$ (**1c**) and $[(\text{NHC})\text{Cu}\{\eta^1\text{-CH}(\text{CH}_2\text{Ph})\text{BPIn}\}]$ (**3**; only the ipso carbon of the phenyl ring of the boron-containing ligand is shown).

DFT calculations (ADF 2000, BP86) performed on complexes **1b** and **1c** are consistent with an $\eta^2(BC)$ -coordination mode. By contrast, calculations on **1a** revealed two different structures of similar energy (within $1.5 \text{ kcal mol}^{-1}$): a singlet $\eta^2(BC)$ -coordinated complex and a triplet $\eta^1(C)$ -coordinated complex (Scheme 2).³⁸ The structural features of the former are similar to those of **1b** and **1c**, while the latter exhibits an expanded Ta–CH₂–B angle of 96° , an elongated Ta–B distance of 2.92 \AA , and a shorter Ta–C distance of 2.34 \AA . Perhaps surprisingly though, the calculated C–B distance in the triplet structure is not substantially elongated relative to that in the singlet species (1.51 versus 1.50 \AA). The reactivity of complex **1a** with alkynes or alkylisocyanides is also consistent with an equilibrium between triplet and singlet state structures in solution. With alkynes, reductive coupling to form metallaboratacyclopentene complexes was observed (Scheme 2), mimicking the reactivity of formally d^2 olefin species such as $[\text{Cp}_2\text{Zr}(\text{CH}_2\text{CHR})]$.⁴⁰ By contrast, with alkylisocyanides (CNCy or CNCH₂Ph), η^3 -

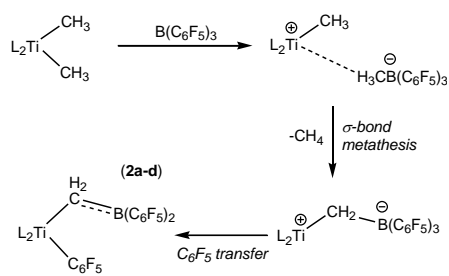
azaallyl products that appear to arise from trapping of $[\text{Cp}_2\text{Ta}\{\eta^1\text{-CH}_2\text{B}(\text{C}_6\text{F}_5)_2\}]$ were isolated; the reaction pathway proposed by Piers and co-workers is provided in Scheme 2.⁴¹



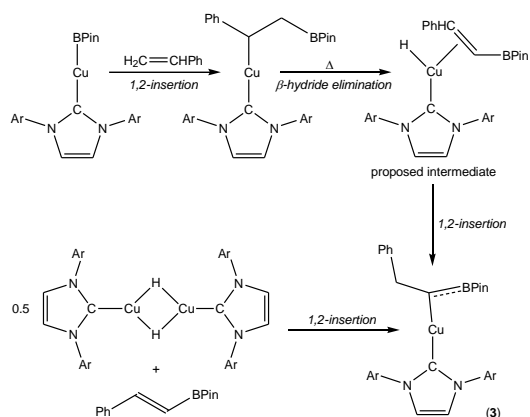
Scheme 2. Calculated singlet and triplet structures of $[\text{Cp}_2\text{Ta}\{\eta^2\text{-H}_2\text{C}=\text{B}(\text{C}_6\text{F}_5)_2\}]$ (**1a**), and the reactions of **1a** with alkynes (C_2Me_2 and HC_2Ph) and isonitriles (CNCy and CNCH_2Ph); dashed reaction arrows signify a proposed reaction pathway.

As highlighted by Piers and Woo, the accessibility of both $\eta^2(BC)$ - and $\eta^1(C)$ -coordination modes for **1a** suggests that η^2 -bonding of the $\text{CH}_2\text{B}(\text{C}_6\text{F}_5)_2$ ligand is fairly tenuous, in part due to the greater electronegativity of carbon versus boron, which emphasizes the contribution of carbon to the occupied molecular orbitals of the ligand. In keeping with this view, a range of d^0 transition metal $[\text{L}_2\text{M}(\text{C}_6\text{F}_5)\{\eta^1(C)\text{-CH}_2\text{B}(\text{C}_6\text{F}_5)_2\}]$ complexes have been reported [e.g. $\text{L}_2\text{M} = \text{Cp}(\text{RO})\text{Ti}$ (**2a**; $\text{R} =$ bulky aryl or silyl),⁴² $\{\text{C}_5\text{H}_4\text{SiMe}_2\text{N}(\text{Xyl})\}\text{Ti}$ (**2b**),⁴³ $\text{Cp}^*(t\text{-Bu}_2\text{C}=\text{N})\text{Ti}$ (**2c**),⁴⁴ and $\{\text{ArN}(\text{CH}_2)_3\text{NAr}\}\text{Ti}$ (**2d**)⁴⁵] exhibiting long $\text{M}-\text{B}$ distances ($> 3.0 \text{ \AA}$) and $\text{M}-\text{C}-\text{B}$ angles in the $111\text{--}125^\circ$ range. These complexes were obtained upon reaction of neutral dimethyl group 4 transition metal complexes with $\text{B}(\text{C}_6\text{F}_5)_3$ as shown in Scheme 3. The related non- d^0 complexes $[(\text{NHC})\text{Cu}\{\eta^1\text{-CH}(\text{CH}_2\text{Ph})\text{-BPin}\}]$ (**3**; Figure 3)⁴⁶ and $[(\text{C}_5\text{R}_5)(\text{CO})_2\text{W}\{\eta^3(\text{CCC})\text{-CH}(\text{Tol})\text{BR}'_2\}]$ $\{\text{R}' = \text{Et}, \text{R} = \text{H}$ (**4a**) and Me (**4b**); $\text{BR}'_2 = \text{BBN} = 9\text{-borylbicyclononane}, \text{R} = \text{H}$ (**4c**); $\text{Tol} = p\text{-tolyl}\}$ ^{47,48} and $[\text{Cp}^*(\text{CO})_2\text{Mo}\{\eta^3(\text{CCC})\text{-CH}(\text{Tol})\text{BEt}_2\}]$ (**4d**)⁴⁹

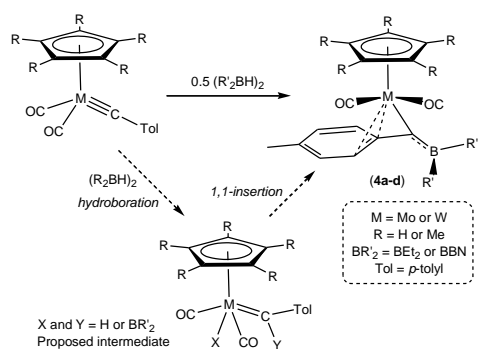
were reported by Sadighi, Stone and Wadepohl, and further highlight the ready accessibility of CR_2BR_2^- coordination modes which do not involve a substantial metal–boron bonding interaction. Copper complex **3** was prepared via the reaction of $[(\text{NHC})\text{Cu}(\text{BPin})]$ with styrene, or alternatively via the reaction of $[\{(\text{NHC})\text{CuH}\}_2]$ (0.5 equivalents) with $E\text{-PhHC}=\text{CH}(\text{BPin})$ (Scheme 4). Group 6 complexes **4a-d** were accessed by reaction of $[(\text{C}_5\text{R}_5)(\text{CO})_2\text{M}(\equiv\text{C-Tol})]$ ($\text{M} = \text{Mo}$ or W) with 0.5 equivalents of $(\text{R}'_2\text{BH})_2$ (Scheme 5).



Scheme 3. General synthesis of $[\text{L}_2\text{Ti}(\text{C}_6\text{F}_5)\{\eta^1\text{-CH}_2\text{B}(\text{C}_6\text{F}_5)_2\}]$ complexes **2a-d**.



Scheme 4. Synthesis of $[(\text{NHC})\text{Cu}\{\eta^1\text{-CH}(\text{CH}_2\text{Ph})\text{BPin}\}]$ (**3**) from $[(\text{NHC})\text{Cu}(\text{BPin})]$ or $[\{(\text{NHC})\text{CuH}\}_2]$ ($\text{Ar} = 2,6\text{-diisopropylphenyl}$).

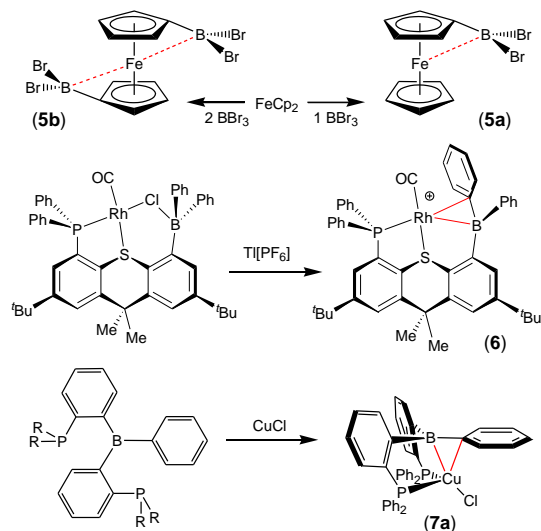


Scheme 5. Synthesis of $[(C_5R_5)_2W\{\eta^3(CCC)\text{-CHPhBR}'_2\}(CO)_2]$ $\{R' = \text{Et}, R = \text{H}$ (**4a**) and Me (**4b**); $\text{BR}'_2 = \text{BBN}, R = \text{H}$ (**4c**) and $[(C_5Me_5)_2Mo\{\eta^3(CCC)\text{-CHPh(BBN)}\}(CO)_2]$ (**4d**).

The metal–boron distances in structurally characterized **4a–c** are greater than 2.9 Å, consistent with an absence of metal–boron bonding. By contrast, the copper–boron distance in **3** is significantly shorter at 2.608(3) Å. However, the ^{11}B NMR chemical shift for **3** (33.4 ppm) differs only slightly from that of $[(\text{NHC})\text{Cu}\{\eta^1(\text{C})\text{-CHPhCH}_2\text{BPin}\}]$ (34.7 ppm; Pin = pinacolate), arguing against any significant Cu–B interaction. Intriguingly though, crystallographically characterized **2a–d**, **3** and **4a–c** exhibit MCHR– BR'_2 bond lengths in the 1.48 to 1.52 Å range, indicative of appreciable B–C double bond character. Furthermore, in all of these complexes, the vacant *p*-orbital on boron is suitably oriented to interact with the lone pair on the α -carbon atom; the angle between the M–C–B plane and the R'–B–R' plane is between 80 and 85° for **2a–b**, **2d**, **3** and **4a–c**, and is 66° in **2c**. In light of the structural attributes of these complexes, it seems reasonable to conclude that the bonding situation in many $\eta^1(\text{C})\text{-CR}_2\text{BR}_2$ complexes (with or without an additional metal–arene interaction as in **4a–c**) is intermediate between the η^1 -borylalkyl and $\eta^1(\text{C})\text{-borataalkene}$ extremes. Although symmetrical η^2 -alkene coordination involving σ -donation and π -backdonation is typically observed in isolable metal complexes, unsymmetrical η^1 -coordination has recently been proposed as a common feature of d^0 metal–alkene complexes. This coordination mode is accompanied by polarization of the C=C bond with a build-up of negative charge on the α -carbon atom and positive charge on the β -carbon atom.⁵⁰ Parallels likely exist between η^1 -alkene and $\eta^1(\text{C})\text{-borataalkene}$ complexes.

The connectivity in Piers' η^2 -borataalkene complexes (singlet **1a** and **1b–c**) is reminiscent of that observed in borylmetallocene complexes such as $[\text{CpFe}\{\text{C}_5\text{H}_4(\text{BBR}_2)\}]$ (**5a**) and $[\text{Fe}\{\text{C}_5\text{H}_4(\text{BBR}_2)\}_2]$ (**5b**) (Scheme 6).⁵¹ The origin of $\text{C}_5\text{H}_4\text{-BR}_2$ bending in borylferrocenes has been studied by Wagner *et al.*, and involves interaction of the $\text{C}_{ipso}\text{-B}$ π -system with a *d*-orbital on iron, in addition to other contributions (direct iron–boron bonding is not involved).⁵² An $\eta^2(\text{BC})$ -coordination mode has also been

observed in Emslie and Bourissou's arylborane complexes $[(\text{TXPB})\text{Rh}(\text{CO})][\text{PF}_6]$ (**6**; ^{11}B NMR δ 57 ppm; cf. 69 ppm in free TXPB),⁵³ $[(\text{PhB}\{\text{C}_6\text{H}_4(\text{PPh}_2)\text{-o}\}_2)\text{CuCl}]$ (**7a**) and $[(\text{PhB}\{\text{C}_6\text{H}_4(\text{P}^i\text{Pr}_2)\text{-o}\}_2)\text{CuCl}]$ (**7b**) (Scheme 6, Figure 4).⁵⁴ The M–B distances in **6** and **7a** are 2.557(3) and 2.396(5) Å, respectively, the M–C_{ipso} bond lengths are 2.362(2) and 2.364(4) Å, and the borane is approximately planar in both cases. Since the B–C distances in these complexes are in the usual range for a B–C_{sp2} single bond, and there is no indication that the aromaticity of the coordinated arene ring has been perturbed, bonding in these complexes can be expected to involve η^1 -borane coordination augmented by an η^1 -arene interaction. DFT calculations on complexes **7a** and **7b** support this picture, but point to the additional importance of interactions between copper and both the B–C σ - and B–C π -orbitals. Investigation of the potential energy surface for complex **7b** also highlighted the presence of multiple energy minima corresponding to structures with significantly different Cu–B and Cu–C_{ipso} distances. This finding is consistent with the observation of two significantly different $\eta^2(\text{BC})$ -coordinated structure types in the unit cell of **7b** ($Z = 4$).



Scheme 6. Synthesis of $[\text{CpFe}(\text{C}_5\text{H}_4\text{BBR}_2)]$ (**5a**), $[\text{Fe}(\text{C}_5\text{H}_4\text{BBR}_2)_2]$ (**5b**),⁵⁵ $[(\text{TXPB})\text{Rh}(\text{CO})][\text{PF}_6]$ (**6**), and $[(\text{PhB}\{\text{C}_6\text{H}_4(\text{PPh}_2)\text{-o}\}_2)\text{CuCl}]$ (**7a**).

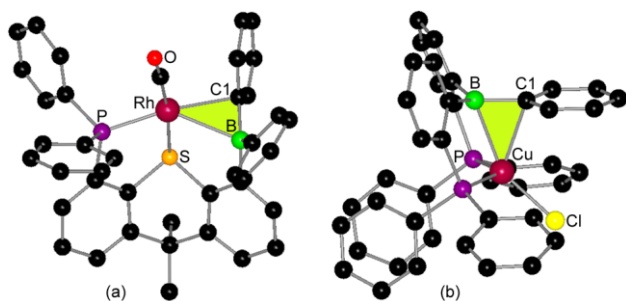


Figure 4. 3 X-Ray crystal structures of: (a) [(TXPB)Rh(CO)][PF₆] (**6**; *tert*-butyl groups and the PF₆ anion are omitted), and (b) [(PhB{C₆H₄(PPh₂)-*o*)}₂CuCl] (**7a**).

3.2. Boraalkene/Azaborataallene Complexes

Allenes are another class of acyclic hydrocarbon π -ligand that is commonly η^2 -coordinated, and while transition metal complexes bearing η^2 -coordinated borataallenes ($R_2C=B=CR_2^-$ or $R_2C=C=BR_2^-$) have not been reported, the coordination chemistry of $\eta^2(BC)$ -coordinated *B*-amino-9-fluorenylideneborane ligands has been explored by Nöth.⁵⁶ These ligands have the potential to behave as boraalkene ($R_2N-B=CR_2$) or zwitterionic azaborataallene ($R_2N=B=CR_2$) ligands, and the latter description appears particularly appropriate. Extended Hückel MO calculations on $H_2N=B=CH_2$ showed four π -molecular orbitals, listed here in increasing energy: (1) a B–N π -bonding orbital (π_{BN}), (2) a B–C π -bonding orbital (π_{BC} ; HOMO), (3) a B–C π -antibonding orbital (π^*_{BC} ; LUMO), and (4) a B–N π -antibonding orbital (π^*_{BN}); Figure 5. In keeping with the greater electronegativity of carbon relative to boron, the HOMO is 87 % localized at carbon, while the LUMO is 80% localized at boron.

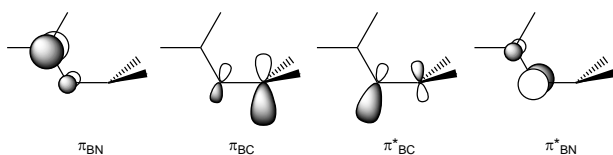
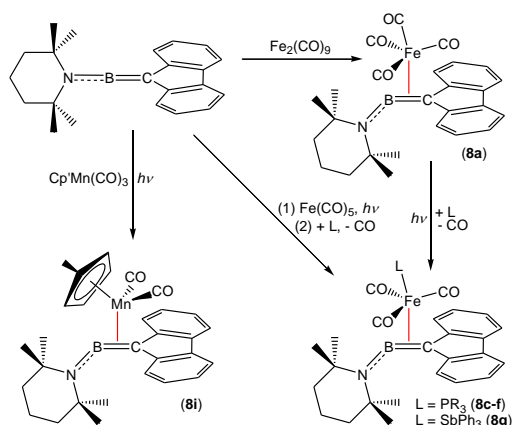


Figure 5. Representation of the π -molecular orbitals of $H_2N=B=CH_2$ (increasing in energy from left to right).

Reaction of *B*-2,2',6,6'-tetramethylpiperidino-9-fluorenylideneborane ($R_2N=B=CAr_2$) with $[Fe_2(CO)_9]$ yielded $[{\eta^2(BC)-R_2N=B=CAr_2}Fe(CO)_4]$ (**8a**) with a distorted trigonal bipyramidal geometry (Scheme 7, Figure 6) and short Fe–B and Fe–C bonds to the $R_2N=B=CAr_2$ ligand {2.125(5) and 2.190(4) Å, respectively}. By contrast, UV irradiation of a mixture of $R_2N=B=CAr_2$ and $[Fe(CO)_5]$ provided $[{\eta^4(BCCC)-R_2N=B=CAr_2}Fe(CO)_3]$ (**8b**) in which the *B*-amino-9-fluorenylideneborane

ligand is bound via the B=C unit and through an η^2 -interaction with the fluorenylidene moiety. Reaction of **8b** with CO provided **8a**, while reaction of **8b** with other neutral Lewis bases, or photolysis of **8a** in toluene in the presence of Lewis bases, provided access to a range of $[\{\eta^2(BC)-R_2N=B=CAr_2\}Fe(CO)_3(L)]$ complexes {e.g. L = PMe₃ (**8c**), PPh₃ (**8d**), P(OMe)₃ (**8e**), PCl₃ (**8f**), and SbPh₃ (**8g**)}. Photolysis of *B*-2,2',6,6'-tetramethylpiperidino-9-fluorenylideneborane with [CpCo(CO)₂], [Cp'Mn(CO)₃] (Cp' = C₅H₄Me) and [(C₆H₆)Cr(CO)₃] also afforded $[\{\eta^2(BC)-R_2N=B=CAr_2\}ML_x]$ {ML_x = CoCp(CO) (**8h**), MnCp'(CO)₂ (**8i**) and Cr(C₆H₆)(CO)₂ (**8j**)} (Scheme 7). Calculations on $[(H_2N=B=CH_2)Fe(CO)_4]$ (a model for compound **8a**) showed that only the π_{BC} and π^*_{BC} ligand orbitals interact strongly with the valence orbitals of the Fe(CO)₄ fragment. The ligand functions both as a donor and as an acceptor, with carbon making the major contribution to the π_{BC} donor orbital and boron making the major contribution to the π^*_{BC} acceptor orbital. The B–C bond length in the free R₂N=B=CAr₂ ligand is 1.420(3) Å, and consistent with the proposed bonding model, the B–C bond lengths in structurally characterized **8a**, **8c**, **8h** and **8i** are significantly elongated, falling in the 1.49(1)–1.53(1) Å range.



Scheme 7. Synthesis of $[\{\eta^2(BC)-R_2N=B=CAr_2\}Fe(CO)_4]$ (**8a**), $[\{\eta^2(BC)-R_2N=B=CAr_2\}Fe(CO)_3L]$ (**8c-g**), and $[\{\eta^2(BC)-R_2N=B=CAr_2\}Mn(CO)_2Cp']$ (**8i**).

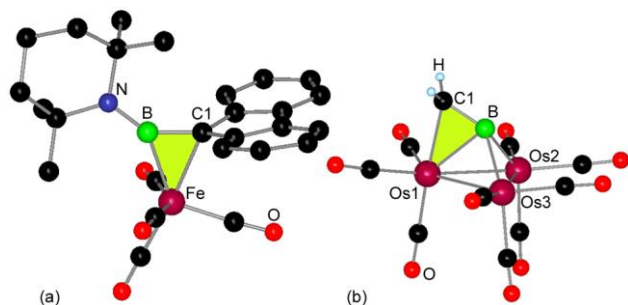
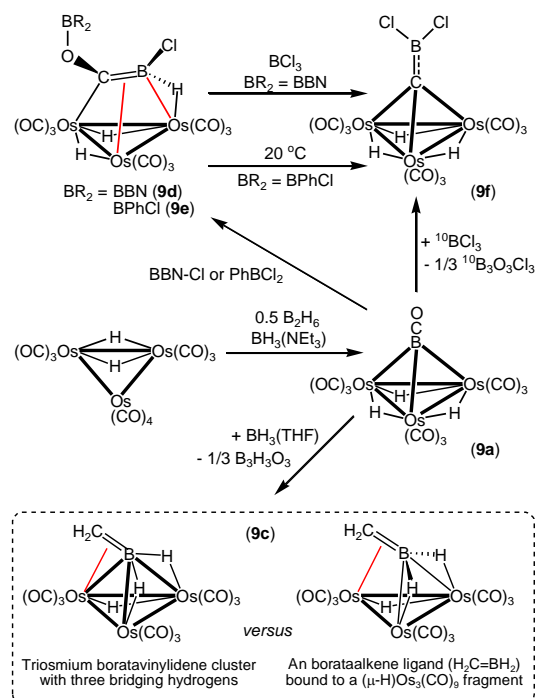


Figure 6. X-ray crystal structures for: (a) [$\{\eta^2(BC)-R_2N=B=CAr_2\}Fe(CO)_4$] (**8a**) and (b) [$(\mu-H)(CO)_9Os_3(\mu_3-H_2B=CH_2)$] (**9c**; only the hydrogen atoms on C(1) were located),

3.3. Multimetallic Complexes Containing $R_2C=BH_2$, $RC=BHR$, $C=BR_2$ and $RC\equiv BR$ Ligands

In 1983, Shore reported the synthesis of the borataketenyliene cluster [$(\mu-H)_3(CO)_9Os_3(\mu_3-BCO)$] (**9a**) from the reaction of $(\mu-H)_2Os_3(CO)_{10}$ with B_2H_6 (0.5 equivalents) and $H_3B(NEt_3)$ (Scheme 8). The linear BCO ligand is unusual in that the C–O distance {1.145(15) Å} and the CO stretching frequency (2120 cm^{-1} ; tentatively assigned) are typical for a CO triple bond, and CO is readily displaced by PMe_3 to yield [$(\mu-H)_3(CO)_9Os_3(\mu_3-BPMe_3)$] (**9b**). However, the B–C distance of 1.469(15) Å in **9a** is consistent with substantial double bond character, and both photoelectron spectroscopy and quantum chemical calculations support this picture.⁵⁷



Scheme 8. Synthesis of complexes **9a** and **9c-9f** (two different representations for the structure of **9c** are shown).

Regardless of the bonding situation in **9a**, reaction of this compound with $BH_3(THF)$ yielded [$(\mu-H)(CO)_9Os_3(\mu_3-H_2B=CH_2)$] (**9c**) which can be viewed either as a borataalkene complex (as in the molecular formula above; see also Scheme 8) or a triosmium boratavinyliene cluster with three

bridging hydrogen atoms ($[(\mu\text{-H})_3(\text{CO})_9\text{Os}_3(\mu_3\text{-B}=\text{CH}_2)]$; Figure 6). The hydrogen atoms on boron were located by ^1H NMR spectroscopy, and in the solid state the following distances were observed: $\text{B}-\text{C}(1) = 1.50(2)$ Å, $\text{B}-\text{Os}(1) = 2.29(1)$ Å, $\text{B}-\text{Os}(2) = 2.27(1)$ Å, $\text{B}-\text{Os}(3) = 2.22(1)$ Å, $\text{C}(1)-\text{Os}(1) = 2.33(2)$ Å. These data are consistent with $\eta^2(\text{BC})$ -coordination to $\text{Os}(1)$, and $\eta^2(\text{BH})$ -coordination to $\text{Os}(2)$ and $\text{Os}(3)$.⁵⁸

In contrast to the reaction of **9a** with $\text{BH}_3(\text{THF})$, reaction of **9a** with $\text{BBN}\text{-Cl}$ or PhBCl_2 yielded $[(\mu\text{-H})_2(\text{CO})_9\text{Os}_3\{\mu_3\text{-C}(\text{OR})=\text{BHCl}\}]$ $\{\text{R} = \text{BBN}$ (**9d**) or BPhCl (**9e**) $\}$ (Scheme 8). These complexes may be viewed as boratavinyl complexes (as in the molecular formula above; see also Scheme 8) or as triosmium borataalkyne clusters with three bridging hydrogen atoms. The X-ray crystal structure of **9d** (Figure 7) revealed a $\text{B}-\text{C}$ distance of $1.46(2)$ Å, $\text{Os}(1)-\text{C}(1)$ and $\text{Os}(2)-\text{C}(1)$ distances of 2.13 and 2.23 Å, and $\text{Os}(2)-\text{B}$ and $\text{Os}(3)-\text{B}$ distances of 2.36 and 2.38 Å, respectively. Based on these parameters, the $\text{C}(\text{OR})=\text{BHCl}$ unit can be considered to be σ -bound to $\text{Os}(1)$, $\eta^2(\text{BC})$ -coordinated to $\text{Os}(2)$, and $\eta^2(\text{BH})$ -coordinated to $\text{Os}(3)$.⁵⁹

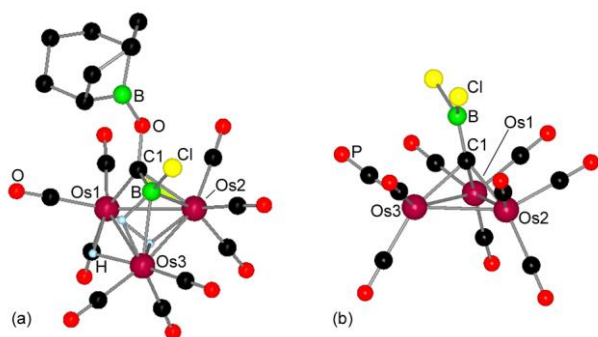
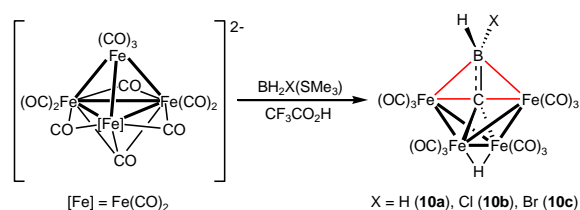


Figure 7. X-ray crystal structures for: (a) $[(\mu\text{-H})_2(\text{CO})_9\text{Os}_3\{\mu_3\text{-C}(\text{O}\{\text{BBN}\})=\text{BHCl}\}]$ (**9d**) and (b) $[(\mu\text{-H})_3(\text{CO})_9\text{Os}_3(\mu_3\text{-C}=\text{BCl}_2)]$ (**9f**; hydrogen atoms were not located).

At room temperature, complex **9e** slowly converted to the boratavinylidene complex $[(\mu\text{-H})_3(\text{CO})_9\text{Os}_3(\mu_3\text{-C}=\text{BCl}_2)]$ (**9f**), which is more straightforwardly accessible through reaction of **9a** or **9d** with BCl_3 (Scheme 8). Labelling studies using $^{10}\text{BCl}_3$ showed that boron in BCl_3 is not incorporated into **9f** on the timescale of the experiment, so the reaction must require intramolecular exchange of the boron and carbon positions relative to the Os_3 cluster core (boron moves from an α -position in **9a** to a β -position in **9f**).⁶⁰ The direct reaction of **9a** with BCl_3 was proposed to proceed via an analogue of compounds **9d** and **9e**. The $\text{B}-\text{C}$ distance in **9f** is $1.47(2)$ Å, suggestive of $\text{B}=\text{C}$ double bond character, but since the $\text{B}=\text{C}$ bond is oriented roughly perpendicular to the Os_3 plane, it cannot engage in η^2 -

coordination to osmium {Figure 7; Os(3)–B = 3.11 Å}. Despite suspected B=C double bond character, boron in complex **9f** is electrophilic, forming labile adducts with NMe₃, PMe₃ and PPh₃. Above –10 °C, the NMe₃ adduct of **9f**, [(μ-H)₃(CO)₉Os₃{μ₃-C–BCl₂(NMe₃)}] (**9g**) was converted to the salt [Me₃NH][[(μ-H)₂(CO)₉Os₃(μ₃-C=BCl₂)] (**9h**); neither of these complexes were crystallographically characterized.⁵⁹

Fehlner and co-workers also reported the synthesis of an iron boratavinylidene complex, [(μ-H)(CO)₁₂Fe₄(μ₄-CBH₂)] (**10a**; ¹¹B NMR δ 10 ppm), via the reaction of [N(PPh₃)₂]₂[Fe₄(CO)₁₃] with excess BH₃(SMe₂), followed by addition of CF₃CO₂H (Scheme 9). In this complex, unlike complex **9f**, the iron atoms adopt a butterfly arrangement, permitting boron to interact with the wingtip iron atoms.⁶¹ Analogous reactions employing BH₂Cl(SMe₂) or BH₂Br(SMe₂) provided access to [(μ-H)(CO)₁₂Fe₄(μ₄-CBHX)] {X = Cl (**10b**; ¹¹B NMR δ 21 ppm) and Br (**10c**)}, reaction of **10a** or **10b** with AlCl₃ provided [(μ-H)(CO)₁₂Fe₄(μ₄-CBCl₂)] (**10d**; ¹¹B NMR δ 30 ppm), and reaction of **10a** or **10c** with AlBr₃ provided [(μ-H)(CO)₁₂Fe₄(μ₄-CBBr₂)] (**10e**). Complexes **10a**, **10b** and **10c** were structurally characterized and have essentially the same structural features (Figure 8). For **10a**, the B–C bond length is 1.574(6) Å, the C(1)–Fe(3) distance is 1.844(1) Å, and the B–Fe(3) distance is 2.427(3) Å. The B–C bond length for **10a** is consistent with a single bond. However, the ¹³C and ¹¹B NMR data for **10a-e** and Fenske-Hall MO calculations are suggestive of some B=C multiple bond character and a significant interaction between the *p*-orbital on boron and the wingtip iron atoms. Consistent with tight coordination of the borane in **10d**, reaction with NEt₃ resulted in deprotonation to form [Et₃NH][[(CO)₁₂Fe₄(μ₄-CBCl₂)] (**10f**) rather than adduct formation, and analogous reactions were observed for **10b** and **10c**.⁶²



Scheme 9. Synthesis of **10a-c**.

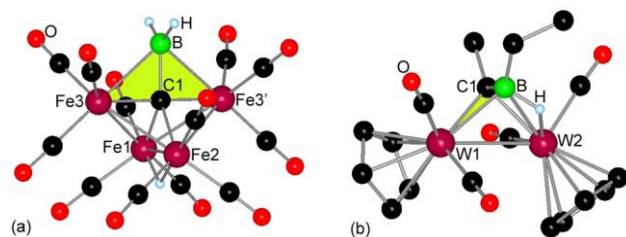
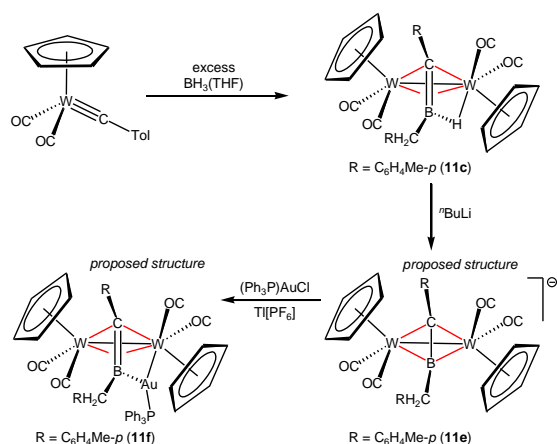


Figure 8. X-ray crystal structures for (a) $[(\mu\text{-H})(\text{CO})_{12}\text{Fe}_4(\mu_4\text{-C}=\text{BH}_2)]$ (**10a**), and (b) $[\{\text{Cp}(\text{CO})_2\text{W}\}_2(\mu\text{-MeC}=\text{BHEt})]$ (**11a**).

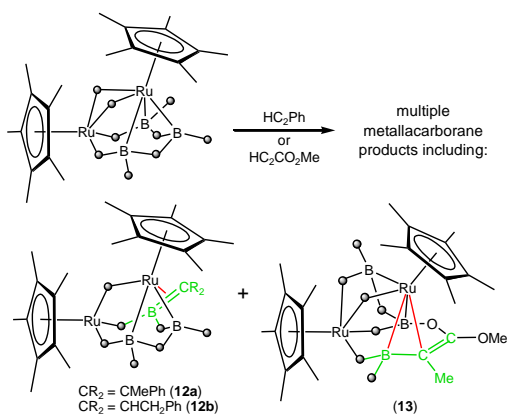
Tungsten boratavinyl complexes similar to triosmium complexes **9d** and **9e** were reported by Stone *et al.*; reaction of $[(\text{C}_5\text{R}_5)(\text{CO})_2\text{W}(\equiv\text{CR})]$ with excess $\text{BH}_3(\text{THF})$ yielded $[\{\text{Cp}(\text{CO})_2\text{W}\}_2(\mu\text{-RC}=\text{BHCH}_2\text{R})]$ $\{\text{R} = \text{Me}$ (**11a**), Ph (**11b**), or $\text{C}_6\text{H}_4\text{Me-}p$ (**11c**) $\}$ and $[\{\text{Cp}^*(\text{CO})_2\text{W}\}_2(\mu\text{-RC}=\text{BHCH}_2\text{R})]$ $\{\text{R} = \text{C}_6\text{H}_4\text{Me-}p$ (**11d**) $\}$ in which the W–W bond is transversely bridged by a $\text{RC}=\text{BHCH}_2\text{R}$ ligand (Scheme 10). The X-ray crystal structure of **11a** (Figure 8) shows a B–C(1) distance of 1.458(1) Å, W–C(1) bonds of 2.14(1) and 2.17(1) Å, and W–B distances of 2.39(1) and 2.41(1) Å. The bridging hydrogen atom was also crystallographically located, and is 1.1(1) Å from boron and 1.8(1) Å from W(2). The bonding situation in this complex is closely related to that in **9d** and **9e**, with $\eta^1(\text{C})$ -coordination to both tungsten atoms, $\eta^2(\text{BC})$ -coordination to W(1), and a B–H–W agostic interaction with W(2). Reaction of **11a** or **11c** with $n\text{BuLi}$ lead to extremely air-sensitive and highly reactive salts presumed to be the $\mu\text{-}\eta^2,\eta^2$ -borataalkyne anions $[\{\text{Cp}(\text{CO})_2\text{W}\}_2(\mu\text{-RCBCH}_2\text{R})]^-$ $\{\text{R} = \text{Me}$ (**11e**) or $\text{C}_6\text{H}_4\text{Me-}p$ (**11f**) $\}$. Subsequent treatment of **11f** with $[\text{AuCl}(\text{PPh}_3)]$ in the presence of $\text{Ti}(\text{PF}_6)_4$ afforded a complex formulated as $[\{\text{Cp}(\text{CO})_2\text{W}\}_2(\mu\text{-RC}=\text{BCH}_2\text{R})\{\text{Au}(\text{PPh}_3)\}]$ ($\text{R} = \text{C}_6\text{H}_4\text{Me-}p$; **11g**), in which the $\text{Au}(\text{PPh}_3)^+$ group is suspected to be located in the position occupied by the proton in **11c** (Scheme 10). However, this unstable complex was not characterized in detail.⁴⁸



Scheme 10. Synthesis of complexes **11c**, **11e** and **11f**.

3.4. Ruthenium metallacarborane clusters

The reaction of *nido*-[1,2-(Cp*RuH)₂B₃H₇] with phenylacetylene was reported by Fehlner *et al.*, and yielded a mixture of metallocarborane clusters including *nido*-[1,2-(Cp*Ru)₂(1,5- μ -CR₂)B₃H₇] {CR₂ = CMePh (**12a**) and CHCH₂Ph (**12b**)}.⁶³ Similar products were formed in the reaction of *nido*-[1,2-(Cp*RuH)₂B₃H₇] with HC₂CO₂Me (Scheme 11 and Figure 9), but in this case, an additional structure type was observed; *arachno*-[1,2-(Cp*Ru)₂{2,8- μ (C)-5- η^1 (O)-CMeCO₂Me}B₃H₇] (**13**).⁶⁴ Clusters **12a-b** and **13** are particularly unusual in that they may, at least from a structural perspective, be considered to contain $\eta^2(BC)$ -coordinated R₂C=BR₂ and R₂C=CR–BR₂ units, respectively. In the context of this review, the most important solid state structural features of these complexes are: (1) a short B(1)–C(1) distance of 1.496(3) Å in complex **12a**, indicative of substantial B=C double bond character and consistent with its formulation as a borataalkene-like complex, (2) a B(1)–C(1) distance of 1.540(4) Å in complex **13**, which is more consistent with a B–C single bond, and (3) a C(1)–C(2) bond distance of 1.399(4) Å in **13**, indicative of a C=C double bond adjacent to boron.



Scheme 11. Formation of complexes **12a-b** and **13** in the reactions of *nido*-[1,2-(Cp*RuH)₂B₃H₇] with phenylacetylene (HC₂Ph) or methyl acetylene monocarboxylate (HC₂CO₂Me). Hydrogen atoms are represented by grey spheres.

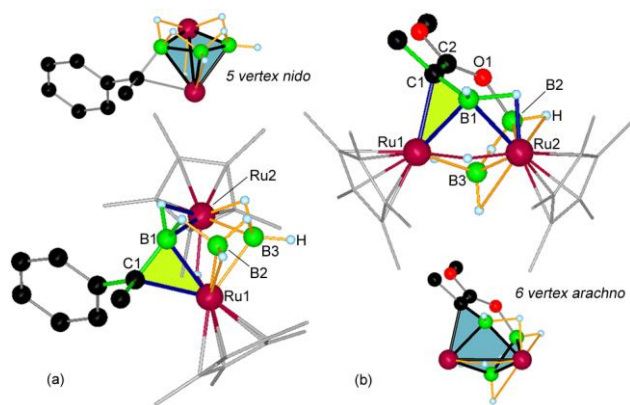


Figure 9. X-ray crystal structures for (a) *nido*-[1,2-(Cp*Ru)₂(1,5-μ-CMePh)B₃H₇] {**12a**; Ru(1)–B(1) = 2.131(2), Ru(1)–C(1) = 2.283(2), B(1)–C(1) = 1.496(3) Å}, and (b) *arachno*-[1,2-(Cp*Ru)₂(3,5-μ-CO₂Me)-3-Me-3-CB₃H₇] {**13**; Ru(1)–B(1) = 2.335(3), Ru(1)–C(1) = 2.275(3), B(1)–C(1) = 1.540(4), C(1)–C(2) = 1.399(4) Å}. Only cluster hydrogen atoms are shown. Larger diagrams emphasize η²(BC)-coordination, while smaller diagrams highlight the metallocarborane cluster core of each molecule.

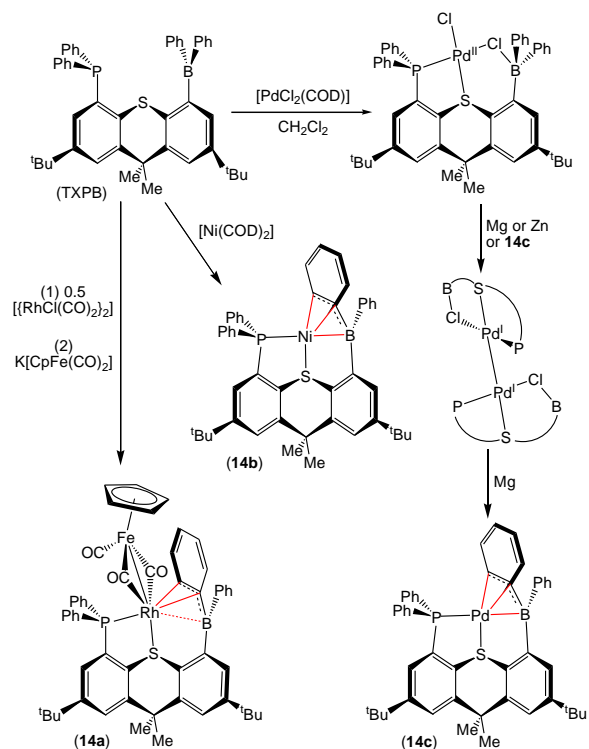
4 Complexes with η³-Coordinated BCC, CBC or BCB Units

4.1 η³-Coordinated Arylborane Complexes

The chemistry of metal–borane complexes (L_xM–BR₃) has advanced greatly over the past 15 years, largely due to the implementation of ambiphilic borane-containing ligands. Research in this area was pioneered by Hill *et al.* using tris(*N*-alkylimazolyl)borane ligands generated in situ via hydride elimination from a coordinated tris(*N*-alkylimazolyl)hydroborate anion.⁶⁵ The chemistry of these and related ligands has been further developed by Hill,⁶⁶ Parkin,⁶⁷ Connelly,⁶⁸ Owen⁶⁹ and others.⁷⁰ Furthermore, the coordination reactivity of isolable borane-containing ambiphilic ligands such as 2,7-di-*tert*-butyl-5-diphenylboryl-4-diphenylphosphino-9,9-dimethylthioxanthene (TXPB),^{53,71–73} R_(3-x)B{C₆H₄(PR'₂)-o}_x (x = 1, 2 or 3),^{54,74,75} 1-(dimesitylboryl)-1'-(diphenylphosphino)ferrocene,⁷⁶ R₂BCH₂CH₂PR'₂,⁷⁷ 2-(picolyl)BCy₂,⁷⁸ Me₂PCMe=CMeBMe₂,⁷⁹ and 8-dimesitylborylquinoline (QuinBMe₂)⁸⁰ has been explored.

While the vast majority of metal–borane complexes exhibit an η¹(B)-coordination mode, the Emslie group's TXPB ligand has proven to be unique in that η³(BCC)-coordination is typically observed via boron and the *ipso*- and *ortho*-carbon atoms of one *B*-phenyl ring. For example, reaction of TXPB with 0.5 [{Rh(μ-Cl)(CO)₂]₂] gave [(TXPB)Rh(μ-Cl)(CO)] featuring a Rh–Cl–BR₃ bridging interaction, and subsequent reaction with K[CpFe(CO)₂] provided heterobimetallic [(TXPB)Rh(μ-CO)₂Fe(CO)Cp]

(**14a**) in which the borane is $\eta^3(BCC)$ -coordinated.⁷² Similarly, reaction of $[Ni(COD)_2]$ with TXPB provided $\eta^3(BCC)$ -coordinated $[Ni(TXPB)]$ (**14b**), and reduction of $[PdCl_2(TXPB)]$ or $[{PdCl(TXPB)}_2]$ with magnesium yielded $\eta^3(BCC)$ -coordinated $[Pd(TXPB)]$ (**14c**)⁷¹ (Scheme 12, Figure 10).



Scheme 12. Synthesis of $[(TXPB)Rh(\mu-CO)_2Fe(CO)Cp]$ (**14a**), $[Ni(TXPB)]$ (**14b**), and $[Pd(TXPB)]$ (**14c**).

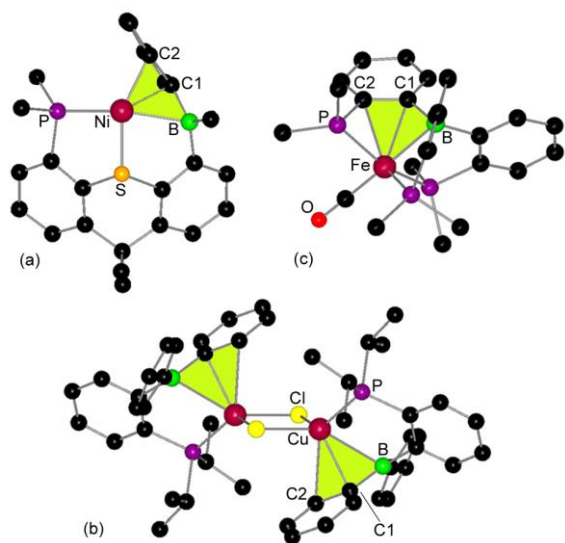
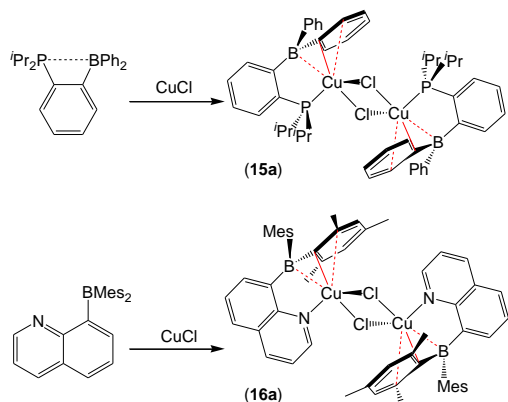


Figure 10. X-ray crystal structures of: (a) $\eta^3(BCC)$ -coordinated [Ni(TXPB)] (**14b**; *tert*-butyl groups are omitted, and only the *ipso* carbon atoms of non-coordinated phenyl rings are shown), (b) $[(\{C_6H_4(BPh_2)(P^iPr_2)-o\}Cu\{\mu-Cl\})_2]$ (**15a**; only isopropyl group methine carbons are shown for clarity), and (c) $[(B\{C_6H_4(P^iPr_2)-o\})_3Fe(CO)]$ (**17**).

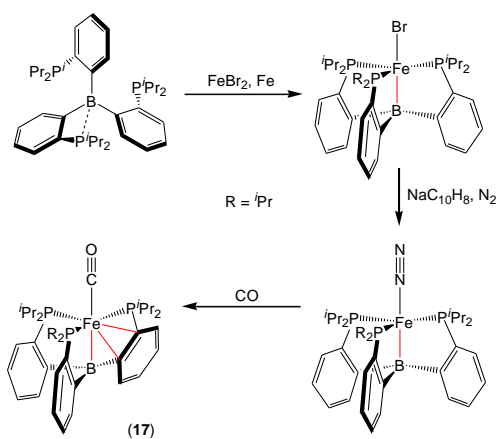
The M–B distances in **14a–c** are 2.63(2), 2.297(4) and 2.320(5) Å, respectively, the M–*C_{ipso}* and M–*C_{ortho}* bond lengths lie in the 2.019(3)–2.46(2) Å range, and the borane is approximately planar. These data are consistent with $\eta^3(BCC)$ -coordination, with stronger metal–boron interactions in **14b** and **14c**. In support of this picture, five independent *CH* signals were observed for the coordinated *B*-phenyl ring in the low temperature ¹H NMR spectra of **14a–c**, and the ¹¹B NMR chemical shifts for **14b** and **14c** are located at lower frequency relative to those for **14a**; 34 and 30 ppm versus 39 ppm, respectively (cf. 69 ppm for free TXPB). DFT calculations (ADF.2005, PW91, TZP) on **14a** confirmed the existence of a significant $\eta^3(BCC)$ -interaction. They also highlighted the presence of significant delocalization within the η^3 -coordinated BCC unit, to the extent that the most appropriate bonding description is intermediate between that expected for an isolated borane/alkene complex and a fully delocalized allyl-like complex.

Recently, $\eta^3(BCC)$ -coordination to copper, silver and iron has been reported by Bourissou,⁵⁴ Hoefelmeyer⁸⁰ and Peters.⁷⁵ Reaction of $C_6H_4(BPh_2)(P^iPr_2)-o$ with CuCl afforded $[(\{C_6H_4(BPh_2)(P^iPr_2)-o\}Cu\{\mu-Cl\})_2]$ (**15a**),⁵⁴ and similarly, reaction of 8-(dimesitylboryl)quinoline (QuinBMes₂) with CuCl or Ag(OTf) yielded $[(\{QuinBMes_2\}Cu(\mu-Cl))_2]$ (**16a**) and $[(\{QuinBMes_2\}Ag(\mu-OTf))_2]$ (**16b**) (Scheme 13).⁸⁰ The Cu–B, Cu–*C_{ipso}* and Cu–*C_{ortho}* distances in complex **15a** (Figure 10) are 2.555(2), 2.339(2) and 2.596(2) Å, and as in complexes **14a–c**, boron is approximately planar and neither the B–*C_{ipso}* or *C_{ipso}*–*C_{ortho}* distances are perturbed from typical values. Interestingly, the phosphine-borane ligand in related $[(\{C_6H_4(BCy_2)(P^iPr_2)-o\}Cu\{\mu-Cl\})_2]$ (**15b**) is $\kappa^1(P)$ -coordinated with a Cu⋯B distance of 3.049(5) Å, perhaps suggesting that the vacant orbital on boron and the π -system of the *B*-phenyl ring play a cooperative role in promoting copper–borane coordination in **15a**. The ¹¹B NMR chemical shifts for complexes **15a** and **15b** are 58 and 82.5 ppm, respectively, supporting the presence of a significant Cu–B interaction in the former. In **16a** and **16b**, longer metal–boron distances of 2.660(3) and 2.902(3) Å were observed, accompanied by M–*C_{ipso}* bond lengths of 2.126(2) and 2.359(3) Å, and M–*C_{ortho}* separations of 2.422(2) and 2.596(3) Å. In both cases, the ¹¹B solution NMR chemical shifts differ only slightly from that of the parent ligand (69 and 72 ppm, respectively, versus 75 ppm), indicative of relatively weak M–B interactions.



Scheme 13. Synthesis of copper complexes $[(\{C_6H_4(BPh_2)(P^iPr_2)-o\}Cu\{\mu-Cl\})_2]$ (**15a**) and $[(\{QuinBMe_2\}Cu(\mu-Cl))_2]$ (**16a**).

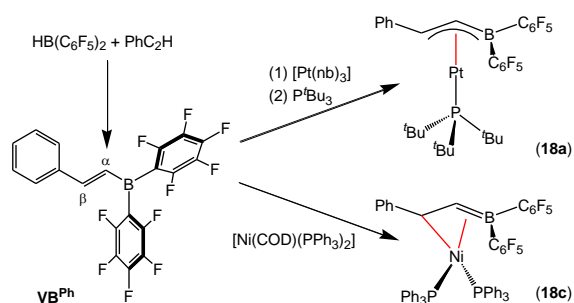
Reaction of $B\{C_6H_4(P^iPr_2)-o\}_3$ with $FeBr_2$ in the presence of excess iron powder afforded $[(B\{C_6H_4(P^iPr_2)-o\}_3)FeBr]$, and subsequent reduction with sodium naphthalenide provided $[(B\{C_6H_4(P^iPr_2)-o\}_3)Fe(N_2)]$, which was converted to $[(B\{C_6H_4(P^iPr_2)-o\}_3)Fe(CO)]$ (**17**) under an atmosphere of carbon monoxide (Scheme 14).⁷⁵ All three phosphorus atoms of **17** are equivalent by NMR spectroscopy at room temperature, consistent with $\kappa^4(BPPP)$ -coordination. However, at low temperature, three mutually coupled ³¹P resonances were observed. The solid state structure of **17** (Figure 10) revealed that the borane unit in the $B\{C_6H_4(P^iPr_2)-o\}_3$ ligand is bound via an $\eta^3(BCC)$ -interaction. Despite the synthesis of a broad range of metallaboratrane complexes over the past 15 years, this is the first example of $\eta^3(BCC)$ -coordination within a metallaboratrane cage structure. The Fe–B, Fe–*C_{ipso}* and Fe–*C_{ortho}* distances in **17** are 2.227, 2.337(2) and 2.321(2) Å, and the sum of the C–B–C angles is 352°. However, it is important to note that these structural parameters will be strongly influenced by the metallaboratrane cage structure.



Scheme 14. Synthesis of $[(B\{C_6H_4(P^iPr_2)-o\}_3)Fe(CO)]$ (**17**).

4.2 η^3 -Coordinated Vinylborane and Borane-Bridged Diylide Complexes

In 2010, Emslie *et al.* reported the reactions of the electrophilic vinylborane E -PhHC=CH-B(C₆F₅)₂ (VB^{Ph})⁸¹ with: (a) [Pt(nb)₃] followed by the addition of 1 equivalent of P^tBu₃, (b) [Pt(nb)(PPh₃)₂], and (c) [Ni(COD)(PPh₃)₂] (Scheme 15). The resulting products, [(^tBu₃P)Pt(VB^{Ph})] (**18a**), [(Ph₃P)₂Pt(VB^{Ph})] (**18b**) and [(Ph₃P)₂Ni(VB^{Ph})] (**18c**), exhibit unsupported $\eta^3(BCC)$ -interactions involving boron and the α - and β -carbon atoms of the vinyl substituent. In **18a-c**, boron is considerably shielded relative to the free ligand, with ¹¹B NMR chemical shifts of 16, 25 and 34 ppm, respectively (versus 58 ppm for VB^{Ph}). These data, in combination with substantial ¹J_{13C;195Pt} (196 and 171 Hz for the β -carbons in **18a** and **18b**), ²J_{13C;13P} (6, 30 and 16 Hz for the β -carbons in **18a-c**), ²J_{1H;195Pt} (40-80 Hz for α -CH and β -CH in **18a** and **18b**), and ⁴J_{19F;195Pt} (78 Hz for the *o*-F atoms of one C₆F₅ ring in **18a**) couplings confirmed η^3 -coordination in solution. However, significant differences were observed in the nature of the metal–vinylborane interactions in structurally characterized **18a** and **18c** (Figure 11).⁸²



Scheme 15. Synthesis of VB^{Ph}, [(^tBu₃P)Pt(VB^{Ph})] (**18a**) and [(Ph₃P)₂Ni(VB^{Ph})] (**18c**).

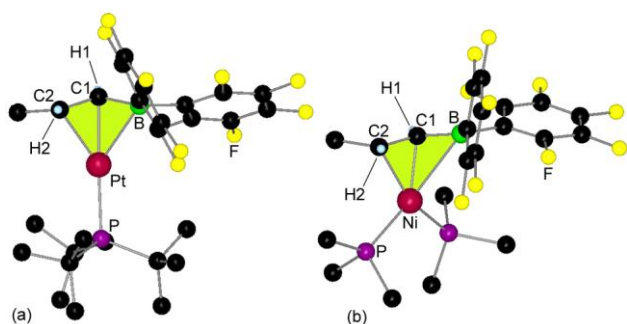


Figure 11. X-ray crystal structures for: (a) $[(t\text{-Bu}_3\text{P})\text{Pt}(\text{VB}^{\text{Ph}})]$ (**18a**) and (b) $[(\text{Ph}_3\text{P})_2\text{Ni}(\text{VB}^{\text{Ph}})]$ (**18c**). Only the *ipso* carbon atoms of phenyl groups on phosphorus or C(2) are shown.

In the solid state structure of **18a** (the unit cell contains 2 independent molecules), short Pt–B_{ave}, Pt–C(1)_{ave}, and Pt–C(2)_{ave} distances of 2.296 Å, 2.128 Å and 2.146 Å were observed. The B–C(1)_{ave} distance of 1.518 Å is slightly shortened relative to that in free vinylboranes, while the C(1)–C(2)_{ave} distance of 1.393 Å is slightly elongated. These data are consistent with allyl-like delocalization within the BCC unit, and in support of this η^3 -borataallyl bonding mode,⁸³ distinctly allyl-like distortions were observed for the substituents on the BCC core; both *exo* substituents {substituents *trans* to the hydrogen atom on C(1)} are bent away from the metal, while the *endo* and central substituents bend towards the metal.^{2,84} DFT calculations (ADF 2008, TZ2P, PW91) confirmed an allyl-like bonding mode with VB^{Ph} acting as both a donor and an acceptor. The HOMO, LUMO and LUMO+1 for the free CH₂CHBH₂ ligand are shown in Figure 12, and are qualitatively analogous to those of an allyl cation, except that the vinylborane LUMO is B–C(1) bonding and C(1)–C(2) antibonding in character. Orbitals on the B–C–C core of VB^{Ph} ligand are analogous to those of the CH₂CHBH₂ model compound.

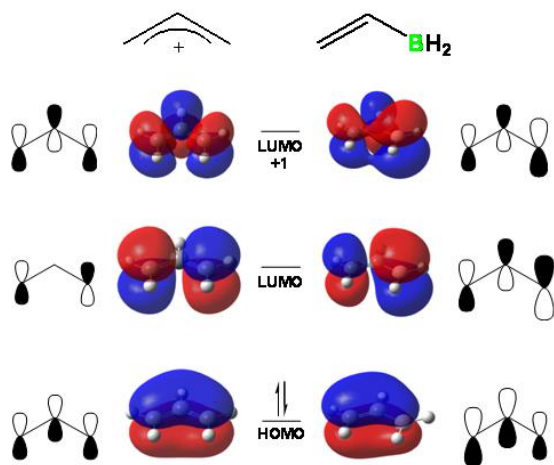
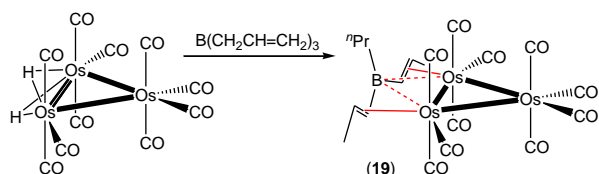


Figure 12. Calculated HOMO, LUMO, and LUMO+1 for an allyl cation ($\text{CH}_2\text{CHCH}_2^+$) and the isoelectronic vinylborane (CH_2CHBH_2).

For complex **18c**, while the spectroscopic data are consistent with $\eta^3(BCC)$ -coordination, several features of the solid state structure are inconsistent with an η^3 -allyl-like coordination mode: (1) short M–C(1) and M–C(2) distances and a relatively long Ni–B distance {2.025(2) and 2.032(2) Å versus 2.660(3) Å}, (2) a short B–C(1) bond and a long C(1)–C(2) bond {1.483(4) and 1.431(3) Å, respectively}, and (3) orientation of both substituents on C(2) away from the metal centre. Instead, these data signify more alkyl/borataalkene-like coordination (Scheme 15) with the borataalkene unit coordinated more tightly at carbon than at boron. This unsymmetrical coordination mode is reminiscent of that observed in Piers' tantalocene borataalkene complexes (**1a-c**). The differences in the vinylborane bonding mode observed for **18a** and **18c** are likely a consequence of both steric and electronic effects; the $\text{Ni}(\text{PPh}_3)_2$ fragment is more bulky and more electron donating than the $\text{Pt}(\text{P}^t\text{Bu}_3)$ fragment.⁸⁵ Consistent with this view, fragment analysis (ADF 2008, TZ2P, PW91) using the fragments $\text{M}(\text{PR}_3)_x$ and VB^{Ph} yielded Hirshfeld charges of -0.255 and -0.404 on the VB^{Ph} fragments of **18a** and **18c**, respectively. These data signify increased electron donation into the VB^{Ph} LUMO in **18c**.

The η^3 -coordination mode in **18a-c** contrasts the η^2 -alkene coordination mode in the previously reported vinylborane complexes $[(\text{CO})_4\text{Fe}\{\text{H}_2\text{C}=\text{CH}-\text{BR}(\text{NMe}_2)\}]$ ($\text{R} = \text{Br}$ and Me),⁸⁶ $[\text{Cp}_2\text{Ti}(\text{ArH}=\text{CH}-\text{BCat})]$ ($\text{Ar} = \text{Ph}$ and $\text{C}_6\text{H}_4\text{OMe-}p$; $\text{Cat} = \text{O}_2\text{C}_6\text{H}_4$ or $\text{O}_2\text{C}_6\text{H}_3^t\text{Bu-4}$),⁸⁷ and $[\text{Cp}^*\text{Ti}(\text{CH}_2=\text{CH}-\text{BO}_2\text{C}_{10}\text{H}_6)]$,⁸⁸ likely due to much greater Lewis acidity of the borane in VB^{Ph} . Related $[(\text{CO})_3\text{Fe}(\text{H}_2\text{C}=\text{CH}-\text{BRNMe}_2)]$ ($\text{R} = \text{Br}$, Me and ^tBu)⁸⁶ and $[(\text{CO})_4\text{Cr}\{^t\text{BuHC}=\text{CH}-\text{BHN}(\text{SiMe}_3)_2\}]$ ⁸⁹ complexes were also reported by Schmid and Braunschweig, but in both cases the vinylborane is η^4 -coordinated and acts as a 4-electron donor; the former is a boron-nitrogen analogue of butadiene, while the latter binds via alkene and σ -borane (M–H–B) interactions. By contrast, Kizas reported the synthesis of $[(\text{CO})_{10}\text{Os}_3\{(E)\text{-MeHC}=\text{CH})_2\text{B}^n\text{Pr}\}]$ (**19**) through the reaction of $[\text{H}_2\text{Os}_3(\text{CO})_{10}]$ with triallylborane (Scheme 16; Figure 13).⁹⁰ The divinylborane ligand in **19** is tightly coordinated via both vinyl groups, and may also engage in some degree of Os–B bonding, given that the B–Os(1) and B–Os(2) distances {2.78(1) and 2.79(1) Å} lie well within the sum of the van der Waals radii.⁹¹ The reported ^{11}B NMR chemical shift of 7 ppm is consistent with 4-coordinate boron and/or substantial B–C multiple bond character. The former seems more likely given that the average B–C_{sp2} bond distance is 1.545 Å, which is in the usual range for a free vinylborane.



Scheme 16. Synthesis of $[(\text{CO})_{10}\text{Os}_3\{(E\text{-MeHC}=\text{CH})_2\text{B}^n\text{Pr}\}]$ (**19**).

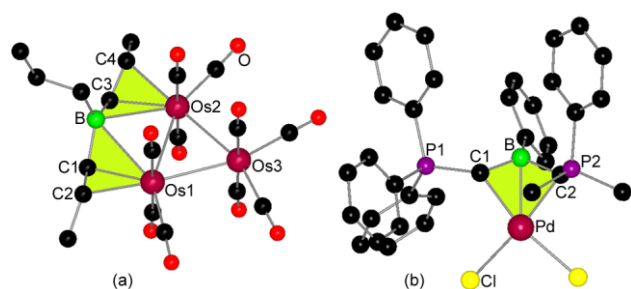
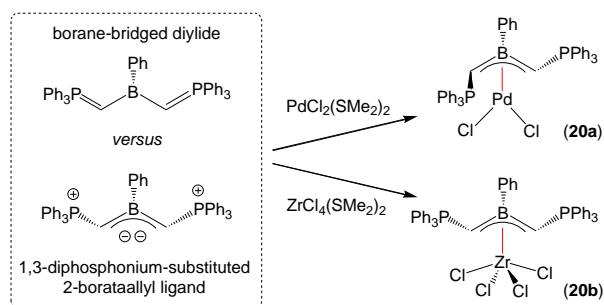


Figure 13. X-ray crystal structures for $[(\text{CO})_{10}\text{Os}_3\{(E\text{-MeHC}=\text{CH})_2\text{B}^n\text{Pr}\}]$ (**19a**) and $[\text{Cl}_2\text{Pd}\{\text{PhB}(\text{CHPPH}_3)_2\}]$ (**20a**; only the ipso carbon atom is shown for two of the phenyl groups on P(2)).

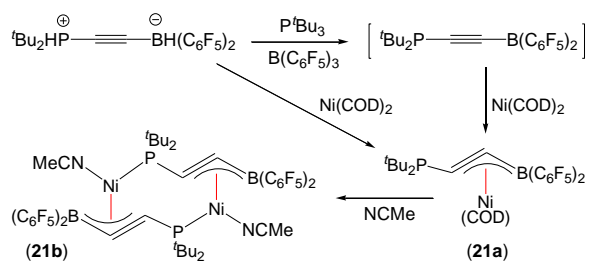
While **18a** is a unique example of a 1-borataallyl-like complex, Shapiro *et al.* have reported the synthesis of the 2-borataallyl-like complexes $[\text{Cl}_2\text{Pd}\{\text{PhB}(\text{CHPPH}_3)_2\}]$ (**20a**) and $[\text{Cl}_4\text{Zr}\{\text{PhB}(\text{CHPPH}_3)_2\}]$ (**20b**) via reaction of $\text{PhB}(\text{CHPPH}_3)_2$ with $[\text{PdCl}_2(\text{SMe}_2)_2]$ or $[\text{ZrCl}_4(\text{SMe}_2)_2]$ (Scheme 17; Figure 13).⁹² The ligand in **20a-b** can be viewed as a borane-bridged diylide or a zwitterionic 1,3-diphosphonium-substituted 2-borataallyl ligand, and PM3 calculations showed that the HOMO and HOMO-1 of the free ligand are qualitatively identical to the corresponding molecular orbitals of an allyl anion. The ¹¹B NMR chemical shifts for **20a** and **20b** are 35 and 33 ppm {cf. 50 ppm for the free $\text{PhB}(\text{CHPPH}_3)_2$ ligand}, consistent with metal-borane coordination and/or significant B-C multiple bond character. The M-C(1), M-B and M-C(2) distances in **20a** are 2.140(4), 2.200(5) and 2.094(4) Å, in keeping with tight η^3 -binding of the ligand. The same metal-ligand bond distances in **20b** {2.434(3), 2.754(4) and 2.469(3) Å} are substantially longer than those in **20a**, but given the larger atomic radius of zirconium relative to palladium, the ligand may still be considered to be $\eta^3(\text{CBC})$ -coordinated. The B-C distances in **20a-b** range from 1.51 to 1.55 Å.



Scheme 17. Synthesis of $[\text{Cl}_2\text{Pd}\{\text{PhB}(\text{CHPh})_2\}]$ (**20a**) and $[\text{Cl}_4\text{Zr}\{\text{PhB}(\text{CHPh})_2\}]$ (**20b**).

4.3 η^3 -Coordinated Alkynylborane and Alkynylboryl Complexes

In 2010, Stephan reported the reaction of zwitterionic ${}^t\text{Bu}_2\text{HP}-\text{C}\equiv\text{C}-\text{BH}(\text{C}_6\text{F}_5)_2$ with the frustrated Lewis pair $\text{B}(\text{C}_6\text{F}_5)_3$ and P^tBu_3 , resulting in $[\text{HP}^t\text{Bu}_3][\text{HB}(\text{C}_6\text{F}_5)_3]$ elimination and formation of thermally unstable ${}^t\text{Bu}_2\text{P}-\text{C}\equiv\text{C}-\text{B}(\text{C}_6\text{F}_5)_2$. While ${}^t\text{Bu}_2\text{P}-\text{C}\equiv\text{C}-\text{B}(\text{C}_6\text{F}_5)_2$ could not be isolated, generation of this compound in the presence of $[\text{Ni}(\text{COD})_2]$ afforded $[\{{}^t\text{Bu}_2\text{P}-\text{C}\equiv\text{C}-\text{B}(\text{C}_6\text{F}_5)_2\}\text{Ni}(\text{COD})]$ (**21a**; ^{11}B NMR δ 7 ppm), which reacted with NCMe to produce $[\{(\mu-{}^t\text{Bu}_2\text{P}-\text{C}\equiv\text{C}-\text{B}\{\text{C}_6\text{F}_5\}_2)\text{Ni}(\text{NCMe})\}_2]$ (**21b**). Complex **21a** was also formed slowly via the direct reaction of ${}^t\text{Bu}_2\text{HP}-\text{C}\equiv\text{C}-\text{BH}(\text{C}_6\text{F}_5)_2$ with $[\text{Ni}(\text{COD})_2]$ (Scheme 18).⁹³ In **21a** (Figure 14), the phosphinoalkynylborane ligand is $\eta^3(\text{BCC})$ -coordinated, while in dimetallic **21b**, it is $\eta^3(\text{BCC})$ -coordinated to one metal centre, and $\kappa^1(\text{P})$ -coordinated to the other. The $\eta^3(\text{BCC})$ -coordination mode of the ${}^t\text{Bu}_2\text{P}-\text{C}\equiv\text{C}-\text{B}(\text{C}_6\text{F}_5)_2$ ligand is very similar in **21a** and **21b**. In **21a**, the Ni–B, Ni–C(1) and Ni–C(2) distances are 2.358(3), 1.987(3) and 2.005(3) Å, and as in the $\eta^3(\text{BCC})$ -coordinated vinylborane complexes **18a-c** and **20a-b**, boron is approximately planar $\{\Sigma(\text{C}-\text{B}-\text{C}) = 358^\circ\}$. At 1.486(4) Å, the B–C(1) bond in **21a** is shortened to the extent that it now lies within the range for isolated borataalkene and borataallene anions. In addition, the C(1)–C(2) bond is considerably elongated $\{1.254(4) \text{ \AA}\}$, and the $\text{C}\equiv\text{C}$ stretching frequency is decreased from 2125 cm^{-1} in zwitterionic ${}^t\text{Bu}_2\text{HP}-\text{C}\equiv\text{C}-\text{BH}(\text{C}_6\text{F}_5)_2$ to 1881 cm^{-1} in complex **21a**. These data are consistent with significant borataallenyl ligand character, paralleling the behaviour of η^3 -coordinated allenyl/propargyl (CR_2CCR) complexes (Figure 15). The substituents on the alkyne (phosphorus and boron) in **21a** are also *trans*-disposed with a B–C(1)–C(2) angle of $156.3(3)^\circ$, falling at the upper end of the usual range for C–C–C angles in allenyl/propargyl complexes ($146\text{--}156^\circ$).⁴ Furthermore, as in allenyl/propargyl complexes, the metal and the η^3 -coordinated unit in **21a** are approximately coplanar. DFT calculations (Gaussian 03, B3PW91, 6-311G**) further support the analogy with allenyl/propargyl ligands, showing π -delocalization over the B–C(1)–C(2) moiety, and Wiberg bond orders of 0.31, 0.17 and 0.40 for Ni–B, Ni–C(1) and Ni–C(2), respectively.⁹³



Scheme 18. Synthesis of $[\{t\text{Bu}_2\text{P}-\text{C}\equiv\text{C}-\text{B}(\text{C}_6\text{F}_5)_2\}\text{Ni}(\text{COD})]$ (**21a**) and $[\{(\mu-t\text{Bu}_2\text{P}-\text{C}\equiv\text{C}-\text{B}\{\text{C}_6\text{F}_5\}_2)\text{Ni}(\text{NCMe})\}_2]$ (**21b**).

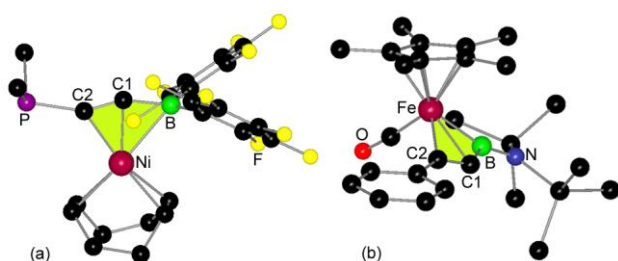


Figure 14. X-ray crystal structures for: (a) $[\{t\text{Bu}_2\text{P}-\text{C}\equiv\text{C}-\text{B}(\text{C}_6\text{F}_5)_2\}\text{Ni}(\text{COD})]$ (**21a**; only the quaternary carbon atoms of the *tert*-butyl groups are shown) and (b) $[\text{Cp}^*(\text{CO})\text{Fe}\{\text{B}(\text{CCPh})\text{N}(\text{SiMe}_3)_2\}]$ (**22**).

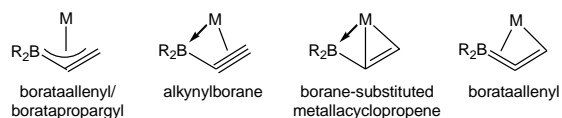
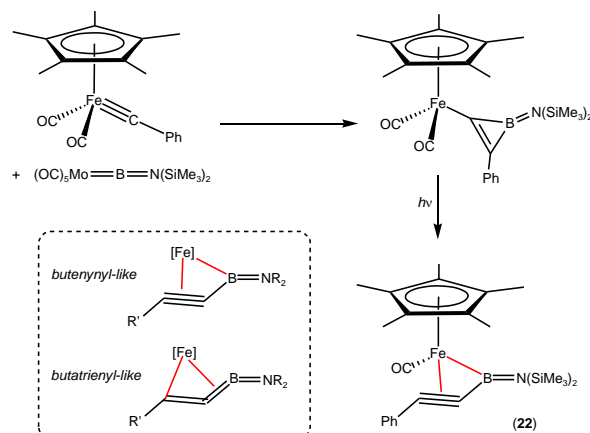


Figure 15. Four possible bonding descriptions for an η^3 -coordinated R_2BCCR ligand.

The reaction of $[\text{Cp}^*(\text{CO})_2\text{Fe}(\text{C}\equiv\text{CPh})]$ with $[(\text{CO})_5\text{Mo}\{=\text{B}=\text{N}(\text{SiMe}_3)_2\}]$ was reported by the Braunschweig group and afforded the iron-substituted borirene complex $[\text{Cp}^*(\text{CO})_2\text{Fe}\{\text{CB}=\text{N}(\text{SiMe}_3)_2\text{CPh}\}]$, which could be converted to $[\text{Cp}^*(\text{CO})\text{Fe}\{\text{B}(\text{CCPh})\text{N}(\text{SiMe}_3)_2\}]$ (**22**) by UV irradiation (Scheme 19).⁹⁴ The BCC-core of the alkynylboranyl ligand in **22** (Figure 14) appears tightly $\eta^3(\text{BCC})$ -coordinated with $\text{Fe}(1)-\text{B}$, $\text{Fe}(1)-\text{C}(1)$ and $\text{Fe}(1)-\text{C}(2)$ distances of 1.995(2), 2.080(2) and 2.040(2) Å, although QTAIM calculations surprisingly did not show a bond path between Fe and C(1). The B–N distance in **22** {1.403(2) Å} is consistent with a B=N double bond, the B–C(1) distance {1.521(2) Å} suggests predominantly single bond character, and the C(1)–C(2) distance {1.268(2) Å} is intermediate between that expected for a double and a triple bond. By analogy with

butatrienyl/butenynyl complexes, the ligand in complex **22** could be viewed as a butatrienyl-like $R_2N=B=C=CPh$ anion or a butenynyl-like $R_2N=B-C\equiv CPh$ anion (Scheme 19), and in this case, the latter description (essentially that of an alkynylboryl ligand) seems most appropriate. The coplanarity of the metal and the η^3 -coordinated BCC-unit is also consistent with a butatrienyl- or butenynyl-like bonding mode, although the B–C(1)–C(2) angle of $134.0(1)^\circ$ is more acute than the C–C–C angles typically observed for the η^3 -coordinated core of allenyl/propargyl or butatrienyl/butenynyl ligands (145 – 156°).^{4,5}

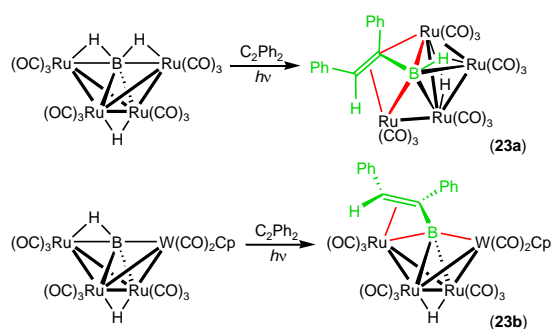


Scheme 19. Synthesis of $[Cp^*(CO)Fe\{B(CCPh)N(SiMe_3)_2\}]$ (**22**). The inset shows possible butatrienyl- and butenynyl-like resonance structures for an $R'C-C-BNR_2$ ligand.

4.4 Cluster Compounds Containing Vinylboryl and Vinylborylene Fragments

Ruthenium clusters containing $BH(CR=CR_2)$ (vinylboryl) and $B(CR=CR_2)$ (vinylborylidene) moieties were reported by Housecroft and co-workers. These complexes, 64-electron $[H(CO)_{12}Ru_4(BHCPHCHPh)]$ (**23a**) and 62-electron $[H(CO)_{11}(CpW)Ru_3(BCPhCHPh)]$ (**23b**), were prepared via photolysis of $[H(CO)_{12}Ru_4(BH_2)]$ and $[H(CO)_{11}(CpW)Ru_3(BH)]$ with diphenylacetylene (Scheme 20).⁹⁵ Cluster **23a** (Figure 16) adopts a spiked triangular tetraruthenium framework, and the boron atom is in contact with all four metal atoms with Ru–B distances of 2.15(1) to 2.24(1) Å. The $HB-CPh=CHPh$ fragment is $\eta^2(BC)$ -coordinated to Ru(1) and $\eta^3(BCC)$ -coordinated to Ru(4) with Ru(1)–C(1), Ru(4)–C(1) and Ru(4)–C(2) distances of 2.39(1), 2.25(1) and 2.18(1) Å. The B–C(1) bond in **23a** lies at the upper end of the range expected for a B–C single bond {1.61(2) Å}, while the C(1)–C(2) bond {1.47(1) Å} is consistent with a π -coordinated olefin moiety. Cluster hydrogen atoms were not crystallographically located, but based on ¹H NMR spectroscopy and the orientation of the carbonyl ligands on each ruthenium atom, the hydrogen atom on boron likely bridges to Ru(2), while the metal hydride is located on the Ru(1)–Ru(3) edge.

Cluster **23b** (Figure 16) retains the tetraruthenium butterfly framework present in the starting material, and the orientations of the ligands on ruthenium are consistent with placement of the bridging hydride along Ru(1)–Ru(2). As in **23a**, boron is bound to all four metal atoms, with a W–B distance of 2.185(9) Å and Ru–B distances between 2.284(8) and 2.395(10) Å. The B–CPh=CHPh fragment is $\eta^3(BCC)$ -coordinated to Ru(3) with Ru(3)–C(1) and Ru(3)–C(2) distances of 2.30(1) and 2.46(1) Å; these distances are significantly longer than those in **23a**. The B–C(1) bond in **23b** is again consistent with a B–C single bond {1.55(1) Å}, while the C(1)–C(2) distance of 1.38(1) Å is indicative of significant C=C double bond character. The shorter C=C bond in **23b** is consistent with less effective coordination of the alkene moiety, as indicated by longer Ru–C(1) and Ru–C(2) distances. However, Fenske-Hall calculations on model compounds for **23a** and **23b** indicated a degree of ambiguity concerning the use of any simple bonding scheme (e.g. Dewar-Chatt-Duncanson bonding of the alkene unit) to describe these molecules.



Scheme 20. Synthesis of $[H(CO)_{12}Ru_4(BHPhCHPh)]$ (**23a**), and $[H(CO)_{11}(CpW)Ru_3(BCPhPhH)]$ (**23b**). The reaction products are drawn to emphasize structural analogies with non-cluster complexes bearing boron-containing π -ligands.

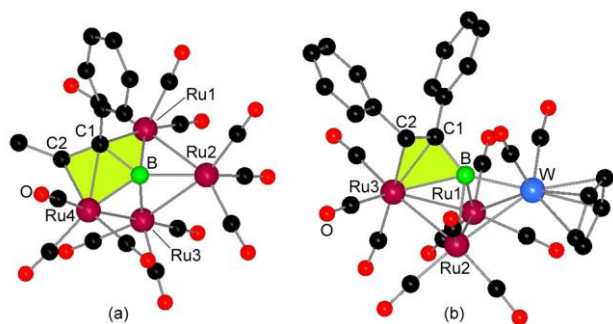
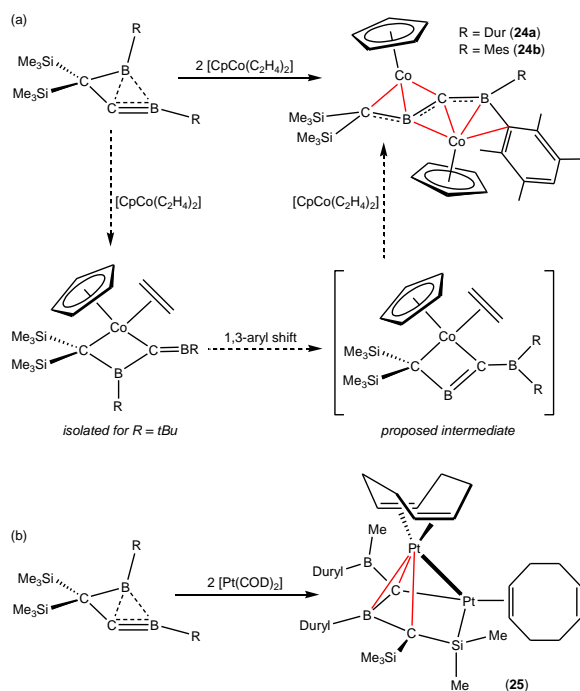


Figure 16. X-ray crystal structures for: (a) $[\text{H}(\text{CO})_{12}\text{Ru}_4(\text{BHCPPhCHPh})]$ (**23a**; only the ipso carbon is shown for the phenyl ring on C(2)) and (b) $[\text{H}(\text{CO})_{11}(\text{CpW})\text{Ru}_3(\text{BCPhCPhH})]$ (**23b**). Cluster hydrogen atoms were not located.

4.5 Diborylcarbene Complexes

Boriranylideneboranes ($\text{RBCR}'_2\text{CBR}$) adopt a unique non-classical structure (Scheme 21), and undergo facile topomerization via a cyclic diborylcarbene intermediate.⁹⁶ In 1995, Siebert and Berndt reported the reaction of $\text{RBC}(\text{SiMe}_3)_2\text{CBR}$ ($\text{R} = \text{Duryl}$ or Mes) with 2 equivalents of $[\text{CpCo}(\text{C}_2\text{H}_4)_2]$. This reaction unexpectedly yielded the dark green bimetallic reaction products $[(\text{CpCo})_2\{(\text{Me}_3\text{Si})_2\text{CBCBR}_2\}]$ ($\text{R} = \text{Duryl}$ (**24a**) and Mes (**24b**)) in which the boron containing ligand is $\eta^3(\text{CBC})$ -coordinated to one metal centre and $\eta^4(\text{BCBC})$ -coordinated to the other. These reactions are proposed to occur via the intermediates in Scheme 21, and in the reaction of $\text{RBC}(\text{SiMe}_3)_2\text{CBR}$ ($\text{R} = \textit{t}\text{Bu}$) with 2 equivalents of $[\text{CpCo}(\text{C}_2\text{H}_4)_2]$, the metallacyclic complex $[\text{Cp}(\text{C}_2\text{H}_4)\text{Co}\{\text{C}(\text{SiMe}_3)_2\text{B}(\textit{t}\text{Bu})\text{C}=\text{B}\textit{t}\text{Bu}\}]$ was isolated, rather than $[(\text{CpCo})_2\{(\text{Me}_3\text{Si})_2\text{CBCB}\textit{t}\text{Bu}_2\}]$ (**24c**) (Scheme 21). The different reaction outcomes with *tert*-butyl versus aryl substituents is likely due to an inability of the *tert*-butyl group to undergo the required 1,3-hydrocarbyl shift.⁹⁷



Scheme 21. Synthesis of: (a) $[(\text{CpCo})_2\{(\text{Me}_3\text{Si})_2\text{CBCBR}_2\}]$ {R = Duryl (**24a**) and Mes (**24b**)} and $[\text{Cp}(\text{C}_2\text{H}_4)\text{Co}\{\text{C}(\text{SiMe}_3)_2\text{B}(\text{tBu})\text{C}=\text{B}'\text{Bu}\}]$, and (b) $\{[(\text{COD})\text{Pt}]_2\{\text{Me}_2\text{SiC}(\text{SiMe}_3)\text{B}(\text{Duryl})\text{C}-\text{BMe}(\text{Duryl})\}\}$ (**25**).

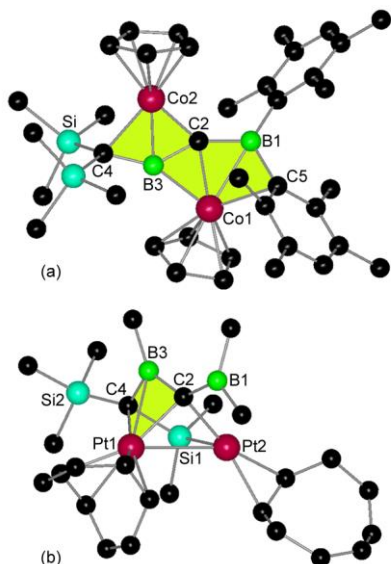


Figure 17. X-ray crystal structures for $[(\text{CpCo})_2\{(\text{Me}_3\text{Si})_2\text{CBCB}(\text{Duryl})_2\}]$ (**24a**) and $\{[(\text{COD})\text{Pt}]_2\{\text{Me}_2\text{SiC}(\text{SiMe}_3)\text{B}(\text{Duryl})\text{CBMe}(\text{Duryl})\}\}$ (**25**; for clarity only the ipso carbon atoms of the two Duryl groups are shown).

The solid state structure of **24a** (Figure 17) revealed that the B(1)–C(2)–B(3)–C(4) chain is significantly bent, but lies in a plane with the two metal atoms. As a result, C(2) is a rare example of a planar tetracoordinate carbon atom. The short Co(1)–C(2) and Co(2)–C(2) distances of 2.009(6) and 1.887(6) Å and the downfield ^{13}C NMR chemical shift for C(2) (195 ppm) are considered to be indicative of significant carbene character. However, extended Hückel and ab initio MO calculations by Gleiter and Siebert *et al.*, which included a fragment analysis using neutral $\{(\text{CpCo})_2\}$ and H_2CBCBH_2 fragments, indicated a unique bonding situation at C(2) with transfer of σ -electron density from Co(1) through C(2) to Co(2) and transfer of π -electron density in the reverse direction.⁹⁸ The remainder of the Co–B and Co–C bonds involving the central boron-containing ligand lie in the 1.973(7) to 2.276(6) Å range, including Co(1)–C(5). At 1.47(1) and 1.48(1) Å, the C(2)–B(3) and B(3)–C(4) distances are consistent with substantial B=C double bond character, and the B(1)–C(2) distance of 1.52(1) Å may suggest some double bond character. Interestingly, electrochemical studies on **24a** showed two reversible reduction waves, one reversible oxidation wave, and a second irreversible oxidation process.

None of the redox products could be isolated, but monoanionic **24a⁻** was detected by EPR spectroscopy at 100 K.

The reaction of (Duryl)BC(SiMe₃)₂CB(Duryl) with 2 equivalents of [Pt(COD)₂] did not yield a structure related to **24a-b**, but instead provided red-orange [(η²-COD)Pt]{(η²;η²-COD)Pt}{Me₂Si-C(SiMe₃)-B(Duryl)-C-BMe(Duryl)}] (**25**), (Scheme 21, Figure 17).⁹⁷ A bond is considered to exist between Pt(1) and Pt(2), and the boron-containing ligand is η³(CBC)-coordinated to Pt(1) and κ²-coordinated to Pt(2) through C(2) and Si(1). The B(3)-C(2) and/or B(3)-C(4) bonds may have some double bond character, but the standard deviations on the bond lengths are too high to draw any informative conclusions.

Conclusions and Outlook

This perspective aims to highlight the diverse range of isolated transition metal complexes bearing η^{*n*}-coordinated (*n* = 2 or 3) acyclic boron-containing π-ligands. These include monometallic, bimetallic and cluster complexes, but for most classes of acyclic boron-containing π-ligand, only a handful of closely related complexes have been prepared. There therefore exists enormous scope for modification of the steric and electronic properties of both the metal fragment (L_{*x*}M) and the boron-containing acyclic π-ligand. In addition, the reactivity of acyclic π-ligand complexes has rarely been explored, despite the potential for development of new transition metal-mediated synthetic pathways to organoboron compounds, by analogy with the chemistry of acyclic hydrocarbon π-ligands, and the possibility, in some cases, for boron and a coordinated metal to interact cooperatively with substrates and/or reaction by-products. A further unique feature of this area is the number of different research fields that have given rise to complexes bearing acyclic boron-containing ligands with the potential for η²- or η³-coordination. These fields include olefin polymerization catalysis, metal-carbon multiple bond hydroboration chemistry, frustrated Lewis pair reactivity, ambiphilic borane ligand coordination chemistry, low valent and small molecule activation chemistry, non-classical boron compound reactivity, metal cluster reactivity, and metallaborane cluster reactivity. Overall, acyclic boron-containing π-ligand chemistry is still at an early stage of development, and future work in this area will no doubt extend and enhance our understanding of the structures and bonding modes accessible for these unique ligands. These advances can be anticipated to promote the rational development of new applications for acyclic boron-containing π-ligands in reactivity and catalysis.

Acknowledgements

D.J.H.E. thanks NSERC of Canada for a Discovery Grant, and the Ontario Ministry of Research and Innovation for an Early Researcher Award. B.E.C thanks NSERC of Canada for a PGS-D scholarship.

Notes and References

- 1 (a) G. E. Herberich, Chapter 5: Boron Rings Ligated to Metals in *Comprehensive Organometallic Chemistry II*, ed. E. W. Abel, F. G. A. Stone, G. Wilkinson, Pergamon Press, Oxford, 1995; vol. 1, pp. 197; (b) R. N. Grimes, Chapter 3.01: Boron-containing Rings Ligated to Metals in *Comprehensive Organometallic Chemistry III*, ed. R. H. Crabtree, D. M. P. Mingos, C. E. Housecroft, Elsevier Ltd., Oxford, 2007; vol. 3, pp. 1.
- 2 C. Elschenbroich, *Organometallics*, 3rd ed., Wiley-VCH, Weinheim, 2006.
- 3 J. F. Hartwig, *Organotransition Metal Chemistry: From Bonding to Catalysis*, University Science Books, Sausalito, California, 2010.
- 4 A. Wojcicki, *Inorg. Chem. Commun.*, 2002, **5**, 82.
- 5 (a) A. K. McMullen, J. P. Selegue and J. G. Wang, *Organometallics*, 1991, **10**, 3421; (b) G. C. Jia, J. C. Gallucci, A. L. Rheingold, B. S. Haggerty and D. W. Meek, *Organometallics*, 1991, **10**, 3459; (c) C. Bianchini, P. Innocenti, M. Peruzzini, A. Romerosa and F. Zanobini, *Organometallics*, 1996, **15**, 272.
- 6 (a) L. G. McCullough, M. L. Listemann, R. R. Schrock, M. R. Churchill and J. W. Ziller, *J. Am. Chem. Soc.*, 1983, **105**, 6729; (b) L. G. McCullough, R. R. Schrock, J. C. Dewan and J. C. Murdzek, *J. Am. Chem. Soc.*, 1985, **107**, 5987.
- 7 The ligand in metallacyclobutadiene complexes is an isomer of that in allenyl/propargyl complexes (CHCHCH versus CH₂CCH), but is coordinated only via the terminal carbon atoms, so is not included in Figure 2. See: (a) M. R. Churchill, J. W. Ziller, L. McCullough, S. F. Pedersen and R. R. Schrock, *Organometallics*, 1983, **2**, 1046; (b) Z. Y. Lin and M. B. Hall, *Organometallics*, 1994, **13**, 2878; (c) F. Erdman and D. B. Lawson, *J. Organomet. Chem.*, 2005, **690**, 4939.
- 8 Relevant van der Waals (and covalent) radii in Å: B 1.92 (0.84), C_{sp2} 1.70 (0.73), Ti 2.07 (1.60), Cr 2.06 (1.39), Mn_{LS} 2.04 (1.39), Fe_{LS} 2.02 (1.32), Co_{LS} 1.91 (1.26), Ni 1.98 (1.24), Cu 1.92 (1.32), Zr 2.19 (1.75), Ta 2.18 (1.70), Mo 2.16 (1.54), W 2.18 (1.62), Ru 2.17 (1.46), Os 2.17 (1.44), Rh 2.04 (1.42), Pd 2.09 (1.39), Pt 2.09 (1.36). LS = low spin. References: (a) M. Mantina, A. C. Chamberlin, R. Valero, C. J. Cramer and D. G. Truhlar, *J. Phys. Chem. A*, 2009, **113**,

- 5806.; (b) S. Nag, K. Banerjee and D. Datta, *New J. Chem.*, 2007, **31**, 832.; (c) B. Cordero, V. Gómez, A. E. Platero-Prats, M. Revés, J. Echeverría, E. Cremades, F. Barragán and S. Alvarez, *Dalton Trans.*, 2008, 2832..
- 9 W. J. Evans, J. L. Shreeve and J. W. Ziller, *Acta Crystallogr. C*, 1996, **52**, 2571.
- 10 M. J. Bayer, H. Pritzkow and W. Siebert, *Eur. J. Inorg. Chem.*, 2002, 2069.
- 11 (a) F. Zettler, H. D. Hausen and H. Hess, *J. Organomet. Chem.*, 1974, **72**, 157; (b) C. D. Good and D. M. Ritter, *J. Am. Chem. Soc.*, 1962, **84**, 1162.
- 12 (a) R. Boese, D. Blaser, N. Niederprum, M. Nusse, W. A. Brett, P. v. R. Schleyer, M. Buhl and N. Hommes, *Angew. Chem. Int. Ed. Engl.*, 1992, **31**, 314; (b) L. H. Toporcer, R. E. Dessy and S. I. E. Green, *Inorg. Chem.*, 1965, **4**, 1649.
- 13 Z. Yuan, C. D. Entwistle, J. C. Collings, D. Albesa-Jové, A. S. Batsanov, J. A. K. Howard, N. J. Taylor, H. M. Kaiser, D. E. Kaufmann, S.-Y. Poon, W.-Y. Wong, C. Jardin, S. Fathallah, A. Boucekkine, J.-F. Halet and T. B. Marder, *Chem. Eur. J.*, 2006, **12**, 2758.
- 14 J. J. Eisch, B. Shafii, J. D. Odom and A. L. Rheingold, *J. Am. Chem. Soc.*, 1990, **112**, 1847.
- 15 K. H. von Locquenghien, A. Baceiredo, R. Boese and G. Bertrand, *J. Am. Chem. Soc.*, 1991, **113**, 5062.
- 16 R. A. Bartlett and P. P. Power, *Organometallics*, 1986, **5**, 1916.
- 17 M. Pilz, J. Allwohn, P. Willershausen, W. Massa and A. Berndt, *Angew. Chem. Int. Ed. Engl.*, 1990, **29**, 1030.
- 18 Y. Sahin, A. Ziegler, T. Happel, H. Meyer, M. J. Bayer, H. Pritzkow, W. Massa, M. Hofmann, P. v. R. Schleyer, W. Siebert and A. Berndt, *J. Organomet. Chem.*, 2003, **680**, 244.
- 19 J. D. Hoefelmeyer, S. Solé and F. P. Gabbai, *Dalton Trans.*, 2004, 1254.
- 20 C.-W. Chiu and F. P. Gabbai, *Angew. Chem. Int. Ed.*, 2007, **46**, 6878.
- 21 M. M. Olmstead, P. P. Power, K. J. Weese and R. J. Doedens, *J. Am. Chem. Soc.*, 1987, **109**, 2541.
- 22 Y. Sahin, M. Hartmann, G. Geiseler, D. Schweikart, C. Balzereit, G. Frenking, W. Massa and A. Berndt, *Angew. Chem. Int. Ed.*, 2001, **40**, 2662.
- 23 M. Pilz, J. Allwohn, R. Hunold, W. Massa and A. Berndt, *Angew. Chem. Int. Ed. Engl.*, 1988, **27**, 1370.
- 24 R. Hunold, M. Pilz, J. Allwohn, M. Stadler, W. Massa, P. v. R. Schleyer and A. Berndt, *Angew. Chem. Int. Ed. Engl.*, 1989, **28**, 781.
- 25 J. Allwohn, R. Hunold, M. Pilz, R.-G. Müller, W. Massa and A. Berndt, *Z. Naturforsch. B*, 1990, **45**, 290.

- 26 B. Glaser, E. Hanecker, H. Nöth and H. Wagner, *Chem. Ber.*, 1987, **120**, 659.
- 27 R. Boese, P. Paetzold and A. Tapper, *Chem. Ber.*, 1987, **120**, 1069.
- 28 P. Willershausen, A. Höfner, J. Allwohn, M. Pilz, W. Massa and A. Berndt, *Z. Naturforsch. B*, 1992, **47**, 983.
- 29 M. Menzel, H. J. Winkler, T. Ablelom, D. Steiner, S. Fau, G. Frenking, W. Massa and A. Berndt, *Angew. Chem. Int. Ed. Engl.*, 1995, **34**, 1340.
- 30 C. Präsang, Y. Sahin, M. Hofmann, G. Geiseler, W. Massa and A. Berndt, *Eur. J. Inorg. Chem.*, 2008, 5046.
- 31 M. Pilz, M. Stadler, R. Hunold, J. Allwohn, W. Massa and A. Berndt, *Angew. Chem. Int. Ed. Engl.*, 1989, **28**, 784.
- 32 R. Boese, P. Paetzold, A. Tapper and R. Ziembinski, *Chem. Ber.*, 1989, **122**, 1057.
- 33 J. Allwohn, M. Pilz, R. Hunold, W. Massa and A. Berndt, *Angew. Chem. Int. Ed. Engl.*, 1990, **29**, 1032.
- 34 W. E. Piers, *Adv. Organomet. Chem.*, 2005, **52**, 1.
- 35 S. Lancaster, *ChemSpider SyntheticPages*, 2001, <http://cssp.chemspider.com/215>.
- 36 C. Lorber, R. Choukroun and L. Vendier, *Organometallics*, 2008, **27**, 5017.
- 37 (a) D. Alberti and K.-R. Pörschke, *Organometallics*, 2004, **23**, 1459; (b) P. Jutzi, C. Müller, A. Stammer and H.-G. Stammer, *Organometallics*, 2000, **19**, 1442; (c) E. Ihara, V. G. Young, Jr. and R. F. Jordan, *J. Am. Chem. Soc.*, 1998, **120**, 8277.
- 38 K. S. Cook, W. E. Piers, T. K. Woo and R. McDonald, *Organometallics*, 2001, **20**, 3927.
- 39 K. S. Cook, W. E. Piers and S. J. Rettig, *Organometallics*, 1999, **18**, 1575.
- 40 K. S. Cook, W. E. Piers and R. McDonald, *J. Am. Chem. Soc.*, 2002, **124**, 5411.
- 41 K. S. Cook, W. E. Piers, P. G. Hayes and M. Parvez, *Organometallics*, 2002, **21**, 2422.
- 42 (a) M. G. Thorn, J. S. Vilaro, P. E. Fanwick and I. P. Rothwell, *Chem. Commun.*, 1998, 2427; (b) A. E. Fenwick, K. Phomphrai, M. G. Thorn, J. S. Vilaro, C. A. Trefun, B. Hanna, P. E. Fanwick and I. P. Rothwell, *Organometallics*, 2004, **23**, 2146; (c) V. Amo, R. Andrés, E. de Jesús, F. J. de la Mata, J. C. Flores, R. Gómez, M. P. Gómez-Sal and J. F. C. Turner, *Organometallics*, 2005, **24**, 2331.
- 43 R. Gómez, P. Gómez-Sal, P. A. del Real and P. Royo, *J. Organomet. Chem.*, 1999, **588**, 22.
- 44 S. Zhang, W. E. Piers, X. Gao and M. Parvez, *J. Am. Chem. Soc.*, 2000, **122**, 5499.
- 45 J. D. Scollard, D. H. McConville and S. J. Rettig, *Organometallics*, 1997, **16**, 1810.
- 46 D. S. Laitar, E. Y. Tsui and J. P. Sadighi, *Organometallics*, 2006, **25**, 2405.

- 47 H. Wadepohl, G. P. Elliott, H. Pritzkow, F. G. A. Stone and A. Wolf, *J. Organomet. Chem.*, 1994, **482**, 243.
- 48 (a) D. Barratt, S. J. Davies, G. P. Elliott, J. A. K. Howard, D. B. Lewis and F. G. A. Stone, *J. Organomet. Chem.*, 1987, **325**, 185; (b) G. A. Carriedo, G. P. Elliott, J. A. K. Howard, D. B. Lewis and F. G. A. Stone, *Chem. Commun.*, 1984, 1585.
- 49 H. Wadepohl, U. Arnold, U. Kohl, H. Pritzkow and A. Wolf, *J. Chem. Soc. Dalton Trans.*, 2000, 3554.
- 50 (a) E. J. Stoebenau, R. F. Jordan, *J. Am. Chem. Soc.* 2006, **128**, 8162 and references therein; (b) F. Sauriol, E. Wong, A. M. H. Leung, I. E. Donaghue, M. C. Baird, T. Wondimagegn, T. Ziegler, *Angew. Chem. Int. Ed.* 2009, **48**, 3342.
- 51 (a) T. Renk, W. Ruf and W. Siebert, *J. Organomet. Chem.*, 1976, **120**, 1; (b) A. Appel, F. Jäkle, T. Priermeier, R. Schmid and M. Wagner, *Organometallics*, 1996, **15**, 1188.
- 52 M. Scheibitz, M. Bolte, J. W. Bats, H.-W. Lerner, I. Nowik, R. H. Herber, A. Krapp, M. Lein, M. C. Holthausen and M. Wagner, *Chem. Eur. J.*, 2005, **11**, 584.
- 53 B. E. Cowie, D. J. H. Emslie, H. A. Jenkins and J. F. Britten, *Inorg. Chem.*, 2010, **49**, 4060.
- 54 M. Sircoglou, S. Bontemps, M. Mercy, K. Miqueu, S. Ladeira, N. Saffon, L. Maron, G. Bouhadir and D. Bourissou, *Inorg. Chem.*, 2010, **49**, 3983.
- 55 W. Ruf, T. Renk and W. Siebert, *Z. Naturforsch. B*, 1976, **31**, 1028.
- 56 (a) S. W. Helm, G. Linti, H. Nöth, S. Channareddy and P. Hofmann, *Chem. Ber.*, 1992, **125**, 73; (b) S. Channareddy, G. Linti and H. Nöth, *Angew. Chem. Int. Ed. Engl.*, 1990, **29**, 199; (c) S. Helm and H. Nöth, *Angew. Chem. Int. Ed. Engl.*, 1988, **27**, 1331.
- 57 (a) J.-H. Chung, E. P. Boyd, J. Liu and S. G. Shore, *Inorg. Chem.*, 1997, **36**, 4778; (b) D.-Y. Jan, D. P. Workman, L.-Y. Hsu, J. A. Krause and S. G. Shore, *Inorg. Chem.*, 1992, **31**, 5123; (c) R. D. Barreto, T. P. Fehlner, L.-Y. Hsu, D.-Y. Jan and S. G. Shore, *Inorg. Chem.*, 1986, **25**, 3572; (d) S. G. Shore, D.-Y. Jan, L.-Y. Hsu and W.-L. Hsu, *J. Am. Chem. Soc.*, 1983, **105**, 5923.
- 58 D.-Y. Jan and S. G. Shore, *Organometallics*, 1987, **6**, 428.
- 59 D. P. Workman, D.-Y. Jan and S. G. Shore, *Inorg. Chem.*, 1990, **29**, 3518.
- 60 D.-Y. Jan, L.-Y. Hsu, D. P. Workman and S. G. Shore, *Organometallics*, 1987, **6**, 1984.
- 61 X. Meng, N. P. Rath and T. P. Fehlner, *J. Am. Chem. Soc.*, 1989, **111**, 3422.
- 62 X. Meng, N. P. Rath, T. P. Fehlner and A. L. Rheingold, *Organometallics*, 1991, **10**, 1986.
- 63 H. Yan, B. C. Noll and T. P. Fehlner, *J. Am. Chem. Soc.*, 2005, **127**, 4831.
- 64 H. Yan, A. M. Beatty and T. P. Fehlner, *J. Am. Chem. Soc.*, 2003, **125**, 16367.

- 65 A. F. Hill, G. R. Owen, A. J. P. White and D. J. Williams, *Angew. Chem. Int. Ed.*, 1999, **38**, 2759.
- 66 (a) M. R. S.-J. Foreman, A. F. Hill, G. R. Owen, A. J. P. White and D. J. Williams, *Organometallics*, 2003, **22**, 4446; (b) I. R. Crossley and A. F. Hill, *Organometallics*, 2004, **23**, 5656; (c) M. R. S.-J. Foreman, A. F. Hill, A. J. P. White and D. J. Williams, *Organometallics*, 2004, **23**, 913; (d) I. R. Crossley, M. R. S.-J. Foreman, A. F. Hill, A. J. P. White and D. J. Williams, *Chem. Commun.*, 2005, 221; (e) I. R. Crossley, A. F. Hill, E. R. Humphrey and A. C. Willis, *Organometallics*, 2005, **24**, 4083; (f) I. R. Crossley, A. F. Hill and A. C. Willis, *Organometallics*, 2005, **24**, 1062; (g) I. R. Crossley, A. F. Hill and A. C. Willis, *Organometallics*, 2005, **24**, 4889; (h) I. R. Crossley, A. F. Hill and A. C. Willis, *Organometallics*, 2006, **25**, 289; (i) I. R. Crossley, A. F. Hill and A. C. Willis, *Organometallics*, 2007, **26**, 3891; (j) I. R. Crossley, M. Foreman, A. F. Hill, G. R. Owen, A. J. P. White, D. J. Williams and A. C. Willis, *Organometallics*, 2008, **27**, 381; (k) I. R. Crossley and A. F. Hill, *Dalton Trans.*, 2008, 201; (l) I. R. Crossley, A. F. Hill and A. C. Willis, *Organometallics*, 2008, **27**, 312; (m) I. R. Crossley, A. F. Hill and A. C. Willis, *Organometallics*, 2010, **29**, 326.
- 67 (a) J. S. Figueroa, J. G. Melnick and G. Parkin, *Inorg. Chem.*, 2006, **45**, 7056; (b) V. K. Landry, J. G. Melnick, D. Buccella, K. Pang, J. C. Ulichny and G. Parkin, *Inorg. Chem.*, 2006, **45**, 2588; (c) K. Pang, S. M. Quan and G. Parkin, *Chem. Commun.*, 2006, 5015; (d) K. Pang, J. M. Tanski and G. Parkin, *Chem. Commun.*, 2008, 1008.
- 68 (a) R. J. Blagg, J. P. H. Charmant, N. G. Connelly, M. F. Haddow and A. G. Orpen, *Chem. Commun.*, 2006, 2350; (b) M. J. López-Gómez, N. G. Connelly, M. F. Haddow, A. Hamilton, M. Lusi, U. Baisch and A. G. Orpen, *Dalton Trans.*, 2011, **40**, 4647; (c) M. J. López-Gómez, N. G. Connelly, M. F. Haddow, A. Hamilton and A. G. Orpen, *Dalton Trans.*, 2010, **39**, 5221; (d) R. J. Blagg, C. J. Adams, J. P. H. Charmant, N. G. Connelly, M. F. Haddow, A. Hamilton, J. Knight, A. G. Orpen and B. M. Ridgway, *Dalton Trans.*, 2009, 8724.
- 69 (a) N. Tsoureas, T. Bevis, C. P. Butts, A. Hamilton and G. R. Owen, *Organometallics*, 2009, **28**, 5222; (b) G. R. Owen, P. H. Gould, A. Hamilton and N. Tsoureas, *Dalton Trans.*, 2010, **39**, 49; (c) G. R. Owen, P. H. Gould, J. P. H. Charmant, A. Hamilton and S. Saithong, *Dalton Trans.*, 2010, **39**, 392.
- 70 (a) D. J. Mihalcik, J. L. White, J. M. Tanski, L. N. Zakharov, G. P. A. Yap, C. D. Incarvito, A. L. Rheingold and D. Rabinovich, *Dalton Trans.*, 2004, 1626; (b) S. Senda, Y. Ohki, T. Hirayama, D. Toda, J.-L. Chen, T. Matsumoto, H. Kawaguchi and K. Tatsumi, *Inorg. Chem.*, 2006, **45**,

- 9914; (c) G. Nuss, G. Saischek, B. N. Harum, M. Volpe, K. Gatterer, F. Belaj and N. C. Möschen-Zanetti, *Inorg. Chem.*, 2011, **50**, 1991.
- 71 D. J. H. Emslie, L. E. Harrington, H. A. Jenkins, C. M. Robertson and J. F. Britten, *Organometallics*, 2008, **27**, 5317.
- 72 S. R. Oakley, K. D. Parker, D. J. H. Emslie, I. Vargas-Baca, C. M. Robertson, L. E. Harrington and J. F. Britten, *Organometallics*, 2006, **25**, 5835.
- 73 D. J. H. Emslie, J. M. Blackwell, J. F. Britten and L. E. Harrington, *Organometallics*, 2006, **25**, 2412.
- 74 (a) M. Sircoglou, S. Bontemps, G. Bouhadir, N. Saffon, K. Miqueu, W. X. Gu, M. Mercy, C. H. Chen, B. M. Foxman, L. Maron, O. V. Ozerov and D. Bourissou, *J. Am. Chem. Soc.*, 2008, **130**, 16729; (b) S. Bontemps, M. Sircoglou, G. Bouhadir, H. Puschmann, J. A. K. Howard, P. W. Dyer, K. Miqueu and D. Bourissou, *Chem. Eur. J.*, 2008, **14**, 731; (c) S. Bontemps, G. Bouhadir, W. Gu, M. Mercy, C.-H. Chen, B. M. Foxman, L. Maron, O. V. Ozerov and D. Bourissou, *Angew. Chem. Int. Ed.*, 2008, **47**, 1481; (d) M. Sircoglou, S. Bontemps, M. Mercy, N. Saffon, M. Takahashi, G. Bouhadir, L. Maron and D. Bourissou, *Angew. Chem. Int. Ed.*, 2007, **46**, 8583; (e) S. Bontemps, H. Gornitzka, G. Bouhadir, K. Miqueu and D. Bourissou, *Angew. Chem. Int. Ed.*, 2006, **45**, 1611; (f) S. Bontemps, G. Bouhadir, K. Miqueu and D. Bourissou, *J. Am. Chem. Soc.*, 2006, **128**, 12056.
- 75 M. E. Moret and J. C. Peters, *Angew. Chem. Int. Ed.*, 2011, **50**, 2063.
- 76 M. W. P. Bebbington, S. Bontemps, G. Bouhadir, M. J. Hanton, R. P. Tooze, H. van Rensburg and D. Bourissou, *New J. Chem.*, 2010, **34**, 1556.
- 77 (a) A. Fischbach, P. R. Bazinet, R. Waterman and T. D. Tilley, *Organometallics*, 2008, **27**, 1135; (b) J. Vergnaud, M. Grellier, G. Bouhadir, L. Vendier, S. Sabo-Etienne and D. Bourissou, *Organometallics*, 2008, **27**, 1140.
- 78 J. Vergnaud, T. Ayed, K. Hussein, L. Vendier, M. Grellier, G. Bouhadir, J.-C. Barthelat, S. Sabo-Etienne and D. Bourissou, *Dalton Trans.*, 2007, 2370.
- 79 J. Grobe, K. Lutke-Brochtrup, B. Krebs, M. Läge, H.-H. Niemeyer and E.-U. Würthwein, *Z. Naturforsch. B*, 2006, **61**, 882.
- 80 J.-H. Son, M. A. Pudenz and J. D. Hoefelmeyer, *Dalton Trans.*, 2010, **39**, 11081.
- 81 D. J. Parks, W. E. Piers and G. P. A. Yap, *Organometallics*, 1998, **17**, 5492.
- 82 K. B. Kolpin and D. J. H. Emslie, *Angew. Chem. Int. Ed.*, 2010, **49**, 2716.
- 83 The term 'borataallyl' is used to describe a BC₂R₅ ligand with a delocalized π -allyl-like bonding mode. It should not be confused with 'borallyl' which refers to the B₃H₇ ligand. .

- 84 R. H. Crabtree, *The Organometallic Chemistry of the Transition Metals*, 3rd ed., John Wiley & Sons, Toronto, 2001.
- 85 T. A. Atesin, S. S. Oster, K. Skugrud and W. D. Jones, *Inorg. Chim. Acta*, 2006, **359**, 2798.
- 86 G. Schmid, F. Alraun and R. Boese, *Chem. Ber.*, 1991, **124**, 2255.
- 87 J. F. Hartwig and C. N. Muhoro, *Organometallics*, 2000, **19**, 30.
- 88 D. H. Motry and M. R. Smith, III, *J. Am. Chem. Soc.*, 1995, **117**, 6615.
- 89 H. Braunschweig, R. D. Dewhurst, T. Herbst and K. Radacki, *Angew. Chem. Int. Ed.*, 2008, **47**, 5978.
- 90 O. A. Kizas, S. Y. Erdyakov, D. Y. Antonov, I. A. Godovikov, E. V. Vorontsov, F. M. Dolgushin, M. G. Ezernitskayaa and I. G. Barakovskaya, *New J. Chem.*, 2009, **33**, 1760.
- 91 (a) M. Mantina, A. C. Chamberlin, R. Valero, C. J. Cramer and D. G. Truhlar, *J. Phys. Chem. A*, 2009, **113**, 5806; (b) S. Nag, K. Banerjee and D. Datta, *New J. Chem.*, 2007, **31**, 832; (c) S. S. Batsanov, *Inorg. Mater.*, 2001, **37**, 871.
- 92 F. Jiang, P. J. Shapiro, F. Fahs and B. Twamley, *Angew. Chem. Int. Ed.*, 2003, **42**, 2651.
- 93 X. Zhao, E. Otten, D. T. Song and D. W. Stephan, *Chem. Eur. J.*, 2010, **16**, 2040.
- 94 H. Braunschweig, Q. Ye, K. Radacki and P. Brenner, *Inorg. Chem.*, 2011, **50**, 62.
- 95 (a) A. K. Chipperfield, B. S. Haggerty, C. E. Housecroft and A. L. Rheingold, *J. Chem. Soc. Chem. Commun.*, 1990, 1174; (b) C. E. Housecroft, J. S. Humphrey, A. K. Keep, D. M. Matthews, N. J. Seed, B. S. Haggerty and A. L. Rheingold, *Organometallics*, 1992, **11**, 4048.
- 96 P. H. M. Budzelaar, P. v. R. Schleyer and K. Krogh-Jespersen, *Angew. Chem. Int. Ed. Engl.*, 1984, **23**, 825.
- 97 (a) A. Gunale, H. Pritzkow, W. Siebert, D. Steiner and A. Berndt, *Angew. Chem. Int. Ed. Engl.*, 1995, **34**, 1111; (b) A. Gunale, D. Steiner, D. Schweikart, H. Pritzkow, A. Berndt and W. Siebert, *Chem. Eur. J.*, 1998, **4**, 44.
- 98 I. Hyla-Kryspin, R. Gleiter, M. M. Rohmer, J. Devemy, A. Gunale, H. Pritzkow and W. Siebert, *Chem. Eur. J.*, 1997, **3**, 294.